THE ASTROPHYSICAL JOURNAL, 321:280–304, 1987 October 1

NEARBY GROUPS OF GALAXIES. II. AN ALL-SKY SURVEY WITHIN 3000 KILOMETERS PER SECOND

R. BRENT TULLY
Institute for Astronomy, University of Hawaii
Received 1986 November 4; accepted 1987 March 17

ABSTRACT

The 2367 galaxies in the Nearby Galaxies (NBG) Catalog have been assigned to clouds, associations, and groups. The group assignments follow from a dendogram analysis with linkages based on an estimator of the gravitational force between entities. The procedure naturally accounts for the effects of tides. Groups are defined by a specific density threshold.

Within the radius of reasonable completion of $25h_{75}^{-1}$ Mpc, 179 groups have been identified that include 69% of the known galaxies and 77% of the light. An additional 20% of the galaxies are in associations and 10% of the galaxies are at-large in clouds. Less than 1% of galaxies are by themselves outside of clouds.

Evidence is presented that the groups are collapsed and that many should be virialized. There is no indication of a serious interloper problem. The properties of the 49 groups with five or more members show less scatter than was the case with previously identified groups. The median virial radius is $340h_{75}^{-1}$ kpc, the median velocity dispersion is 100 km s^{-1}, and the median value of $M_V/L_B^{b,i}$ is $94h_{75}$ $M_\odot/L_\odot$. Intrinsic scatter about this M/L value is less than or about a factor of 2 rms.

This substantial median M/L value must be characteristic of the average galaxy. Apparently, mass increasing roughly linearly with radius out to a few hundred kiloparsecs is the norm for galaxies and a rather firm lower limit of $\Omega_g = 0.08$ can be given as the fraction of closure density directly associated with galaxies.

Subject heading: galaxies: clustering

I. INTRODUCTION

Seven years have gone by since the publication of Paper I in this series (Tully 1980). During the earlier investigation, it became evident that there is a significant deficiency in the way groups of galaxies have been identified, and it has taken until now to come to terms with the problem. The difficulty has been that groups have been identified in ignorance of the larger scale structure that contains them. A more ambitious analysis is now possible because of the material that is published in the *Nearby Galaxies Atlas* (Tully and Fisher 1987, hereafter NBG atlas) and the accompanying *Nearby Galaxies Catalog* (Tully 1987, hereafter NBG catalog). The atlas displays the two- and three-dimensional distribution of an all-sky sample of 2367 galaxies with $V_0 < 3000$ km s^{-1}.

With the atlas available, it is possible to dissect the large-scale structure into smaller scale units. Specifically, we are able to provide a three-tiered description of the environment of every galaxy in our sample. On the largest scale, we identify the *cloud* that a galaxy lies in. On the smallest scale, we specify if the galaxy lies in a *group* on the basis of a rigorous algorithm. On an intermediate scale, we link groups and individual galaxies into *associations*.

The present analysis incorporates one other instructive feature. The influence of gravity is considered, both from the obvious standpoint of the force of attraction and from the more subtle standpoint of tidal disruption. There is good evidence that tidal action plays a major role on the scale of groups in the environment of the Local Supercluster.

II. THE SAMPLE

We consider the 2367 galaxies in the NBG catalog. This catalog contains all galaxies that were known to have a systemic velocity less than 3000 km s^{-1} when entry of new members to the catalog was essentially terminated circa 1980. The characteristics of the sample are dominated by two contributing sources. All Shapley-Ames (1932) galaxies within the velocity cutoff are included (1053 galaxies: Sandage 1978; Sandage and Tammann 1981), which assures completion across the sky to $B_T^{b,i} \approx 12.0$. In addition, the results of an all-sky H I survey are included.

The H I survey was conducted after the author compiled a list of candidate nearby galaxies upon a complete reinspection of the Palomar Observatory Sky Survey and the European Southern Observatory Quick Blue Survey. A description of the selection criteria and the results of observations made from the northern hemisphere are given by Fisher and Tully (1981). Reif *et al.* (1982) observed those candidate galaxies in the southern sky that also appear in the *Second Reference Catalogue* (de Vaucouleurs, de Vaucouleurs, and Corwin 1976). Observations of the remaining southern galaxies will be discussed by Chamaraux *et al.* (1999). These three sources provide 1515 redshifts to the NBG catalog, with some overlap with the Shapley-Ames sample.

The Shapley-Ames sample provides completion to a specific magnitude limit. The H I survey provides information about low surface brightness, gas-rich systems that are the major visible constituents of the present universe outside of clusters. The completion characteristics of the H I survey are described by Fisher and Tully (1981), but, in summary, there is good completion for types Sc and later to a specified size limit for systemic velocities less than 1500 km s^{-1}, with significant deficiencies occurring above 2000 km s^{-1}. An important point for the present discussion is that the NBG catalog provides relatively *uniform* coverage of the entire unobscured sky.

Several major redshift surveys have been published since our cutoff date and are not included; most notably the CfA survey (Huchra *et al.* 1983). If the recent major surveys had been

included, the sample could have been significantly expanded in selected parts of the sky, but the virtue of uniform coverage across the sky would have been lost.

III. GROUP ASSIGNMENTS

a) Clusters

The major concentrations of galaxies within 3000 km s^{-1} were identified in the course of the construction of the NBG atlas. The concern in that context was to eliminate the most obvious "finger of God" effects in maps that involve the velocity dimension. There are 13 condensed groups with at least five members that would appear significantly elongated in the redshift direction if no correction were made. These 13 cases are identified in Table 1.

These aglomerations we call clusters, while smaller entities will be called groups. These high-dispersion clusters have been picked out by hand because, without them to consider, it reduces the complexity of the algorithm that will subsequently be used to pick out groups.

b) General Considerations Regarding the Definition of Groups

The first extensive group catalog was published by de Vaucouleurs (1975). The criteria for group selection in that work were qualitative. Entities were identified that seemed to stand out on the sky, in velocity, by morphological characteristics, and by apparent magnitude. However, in that work there was no precise notion of what was implied in terms of overdensity with respect to the background or any preconceived ideas of the scale of groups or their velocity dispersions. This approach was appropriate for a first consideration of the problem.

Subsequently, attempts were made to be more quantitative in the definition of groups. Turner and Gott (1976) specified groups on the basis of an overdensity criterion on the plane of the sky. Huchra and Geller (1982, hereafter HG) and Geller and Huchra (1983, hereafter GH) applied a similar criterion to define groups in three dimensions, making use of velocities. These latter authors had the extensive CfA redshift survey at their disposal.

TABLE 1

THIRTEEN CLUSTERS

Common Name (1)	Group (2)	Number (3)	V_p (4)	R_V (5)	$M_V/L_B^{b,i}$ (6)
*Virgo	11–1	130	715	0.79	562
Virgo W	11–24	12	311	0.48	184
*Ursa Major	12–1	57	148	0.98	95
*Coma I	14–1	25	266	0.34	523
*M96	15–1	9	112	0.14	92
Antlia	31–2	7	479	0.11	434
NGC 5846	41–1	11	344	0.27	214
NGC 5371	42–1	15	162	0.59	36
*Fornax	51–1	31	434	0.32	431
*NGC 1332	51–4	17	110	0.50	87
*NGC 1566	53–1	13	236	0.29	319
NGC 6868	61–1	5	133	0.16	29
NGC 6707	61–4	5	172	0.16	74

COL. (1).—Name of cluster. Asterisk indicates cluster is in region of reasonable completion with distances $<25h_{75}^{-1}$ Mpc.

COL. (2).—Group number in Table 2.

COL. (3).—Number of known cluster members.

COL. (4).—"Probable" dispersion, corrected for observational uncertainties, in km s^{-1}.

COL. (5).—Virial radius in h_{75}^{-1} Mpc.

Col. (6).—Mass-to-light ratio, in solar units.

These quantitative selection processes are meritorious, but they suffer some deficiencies. For one thing, as applied, there has been a tendency to merge units along the line of sight that are probably unbound neighbors within filamentary structure. For another, depending on the selection algorithm, these methods can be insensitive to extended, low density contrast groups. Also, although it is not the fault of the methods, they have been applied to samples that are poorly represented by low mass systems, and consequently, define groups that are different in characteristics from those seen very nearby.

Materne (1978, 1979) introduced the concept of the dendogram to group analysis, whereby one takes a sample of galaxies and then links them on the basis of some property, such as their separations. One starts with all the galaxies as separate units and links them in order of the optimization of a chosen property until there is only one unit that encompasses the ensemble. This method was explored in Paper I. Rood (1983) has subsequently used it to study the clustering of nearby stars, and Vennik (1984), to study the clustering of galaxies.

For reasons described more completely in Paper I, the property we chose to optimize (in this case, maximize) with each linkage is luminosity divided by separation squared. Evidently, this parameter is related to the force of attraction between two units if mass and light are coupled. Vennik (1984) followed a similar procedure and used a sample with substantial overlap with ours, though that work was confined to the northern hemisphere. There are differences in the way separations are defined, and Vennik used a number density rather than a luminosity density isolation criterion. Our method is described in the following subsections.

c) Separations

The criticism by HG that in Paper I we constrained velocity dispersions to be small through our linkage between information on the plane of the sky and in the line of sight reveals a misunderstanding on their part concerning what we did previously. There is no need to dwell on that point, though, because the one major advance in our methodology since Paper I concerns a new procedure for the derivation of separations.

We now presume that there are two limiting regimes and prescribe a recipe to handle intermediate situations. In the limit of *large* differences in systemic velocities we assume that differential velocities are simply related to the expansion of the universe and directly infer a line-of-sight separation. In this limiting case, separations are taken to be the vector sum of the observed plane-of-sky and inferred line-of-sight components. In the limiting case of *small* differences in systemic velocities we assume that there is *no information* about line-of-sight separations in the differential velocities. In this limiting case, separations are taken strictly from plane-of-sky information, with the geometric correction factor $4/\pi$ applied to correct statistically for depth in the third dimension. For intermediate cases, we adhere to an algorithm that transforms between the limiting cases in a smooth way. The process is regulated by the choice of a single free velocity parameter: for velocity differentials less than the value of this parameter, one is in the regime of the low-velocity limiting case.

If the limiting differential velocity parameter is V_l, then separations R_{ij} are derived according to the following expressions:

If $V_{ij} \leq V_l$,

$$R_{ij} = (8/\pi)D \sin(\theta_{ij}/2) . \quad (1a)$$

If $V_{ij} > V_l$,

$$R_{ij} = \{4D^2 \sin^2 (\theta_{ij}/2)[1 + (4/\pi - 1)V_l^2/V_{ij}^2]^2 + (V_{ij}^2 - V_l^2)/H_0^2\}^{1/2} . \quad (1b)$$

In the limit $V_{ij} \gg V_l$,

$$R_{ij} \approx \{[2D \sin (\theta_{ij}/2)]^2 + (V_{ij}/H_0)^2\}^{1/2} . \quad (2)$$

In these equations, V_{ij} is the radial velocity differential between galaxies i and j, θ_{ij} is the angular separation between them, and D is the average of the two individual galaxy distances based on their velocities, a Virgocentric retardation model (Tully and Shaya 1984), and $H_0 = 75$ km s^{-1} Mpc^{-1}.

If V_l is chosen too *small*, then there will be a tendency to derive separations that are too big because the peculiar velocities of galaxies will be interpreted as implying large separations. In this case, the trend would be to reject honest members with large peculiar velocities and, consequently, to *underestimate* the velocity dispersion of groups. If V_l is chosen too *big*, then there will be a tendency to include galaxies into groups that are only accidental superpositions in the line of sight. In this case, nonmembers with Hubble expansion components to their differential velocities will be included and, consequently, the trend will be to *overestimate* the velocity dispersion of groups. These considerations are similar to those that concerned HG in their choice of the parameter they call V_0.

Fortunately, it turns out to be possible to choose a value of V_l that minimizes the aforementioned problems. The situation is ameliorated by the fact that the 13 most obvious clusters have already been picked out. Hence, it is not necessary to choose V_l to accommodate the likes of, say, the Virgo Cluster. We only need V_l large enough to handle the groups that are less prominent than the most obvious 13.

After some experimentation, $V_l = 300$ km s^{-1} was chosen as optimum. In the analysis to be described, this value of V_l was used unless there was a compelling reason to choose a different value. In a statistically insignificant number of cases (roughly 3% of cases) V_l was decreased to as low as 200 km s^{-1} or increased to as much as 400 km s^{-1}. For example, V_l was decreased in the case of the NGC 1023 group because we still feel that the conclusion of Paper I is valid that UGC 2080 is to the background.

It is to be emphasized that the choice of $V_l = 300$ km s^{-1} is very robust, for the same reasons that HG found their results to be insensitive to the value of their V_0. A change of ± 100 km s^{-1} does not modify the results of the analysis in the substantial majority of cases. The results of the objective group definitions were considered subjectively in all cases and only rarely was there reason for reconsideration. In any event, galaxies that are good candidates for group membership but that are ultimately rejected do not get lost because they inevitably are recorded as "associated."

d) Tidal Disruption

The composition of identified groups is actually more strongly affected by another characteristic of the analysis than by the choice of V_l. Tidal effects must be very important. From an analysis of the environment of a group that ignores the influence of neighbors, it might be concluded that outlying galaxies are loosely bound to the prospective group, but, in reality, the outlying galaxies might be bound to a more distant but more prominent entity.

Given our present knowledge, the obvious way to proceed is to assume that mass is distributed like light and, hence, to take the gravitational influence of each component to be proportional to its luminosity. If the luminosity of a galaxy in the sample is unknown, then an approximate value can be calculated based on the size of the galaxy and an assumed mean surface brightness.

The influence of tidal effects can be judged by repeating an analysis, in one instance with the influence of adjacent clusters felt in proportion to their luminosities and, in another instance, with the influence of adjacent clusters "turned off." Only linkages that survive when the effect of the clusters is considered are to be identified as "groups," while galaxies that are linked only in the abeyance of the influence of nearby clusters are identified as "associated."

e) Groups

We can now specify our criterion for the identification of a group. Suppose we begin with a sample of N individual galaxies. We consider all pairwise combinations and link the pair that has the maximum value of LR_{ij}^{-2}, where L is the luminosity of the brighter component and R_{ij} is the separation. The connected pair is now viewed as a single entity located at the barycenter of the separate components and with the sum of the luminosities of the components. There are now $N - 1$ separate units to consider and the process is repeated. After $N - 1$ steps, all galaxies have been incorporated into one unit.

As in Paper I, we chose to define membership, not on the basis of the value of LR_{ij}^{-2}, but on the basis of the *density* of the entity, measured by $\rho = LR_{ij}^{-3}$. If there is a universal value of the mass-to-light ratio, then it could be imagined that a value of ρ could be specified such that units with higher values have collapsed by the present epoch while units with lower values have *not* collapsed.

It remains for us to specify the critical value of ρ. After the evaluation of a few dozen cases, we became convinced that this critical value is rather well constrained, with an uncertainty of only a factor of 2 or so. The bases for this statement are (1) the regions around groups frequently have a core-halo appearance, and densities in the outer parts of cores are rather consistent; and (2) the groups must pass a crossing-time test. The desired critical density value should define groups that have crossing times less than the age of the universe. Smaller density values should tend to define groups with crossing times longer than the age of the universe. We settle on the value $\rho_g = 2.5 \times 10^9\ L_\odot$ Mpc^{-3}. Hence, a companion galaxy 1 Mpc from an entity with $2.5 \times 10^9\ L_\odot$ would be accepted as a group member, as would be a system 2 Mpc from an entity 8 times brighter.

This limiting density is determined by empirical considerations and is soft by at least a factor of 2. In particular, we regret that we chose to use only the luminosity of the brighter unit in calculating ρ rather than the sum of the two components in a linkage. The difference is usually small but could be as much as a factor of 2. To be precise, we rigorously adhere to the specified limiting value. We have not yet checked the effect a different choice would have on the inferred properties of groups, but we suspect that it will be minor for any reasonable value of ρ_g.

Our limiting density parameter is more easily interpreted than the density contrast parameters defined by Turner and Gott (1976), HG, and GH. Our parameter is strictly defined by conditions *within* the prospective group,[1] rather than in con-

[1] Except in special circumstances near to major clusters where it can be inferred that groups are being tidally disrupted.

trast with an average density. It remains to be demonstrated that the groups that have been identified really have collapsed or, indeed, are even bound.

f) Associations

A special feature of the present analysis is the identification of linkages on several scales. In particular, we identify "associations" of galaxies.

The motivation for the introduction of this descriptive terminology is the observation that many groups appear to have a core-halo morphology. It is very common to find an overdensity of galaxies in the region surrounding entities that satisfy the group criterion of the previous section (see Fig. 13 in Appendix B). However, the more tenuously linked galaxies have group crossing times in excess of the age of the universe and could only be bound if mass-to-light ratios are much higher than commonly accepted.

There is reason to believe that the more distantly associated galaxies are *not* bound. It was mentioned in the subsection on tidal disruptions that tests made with the effects of nearby clusters "on" and "off" reveal that the halos about groups are very susceptible to tidal dislocation. In the past, galaxies would have been closer together in general, and the situation for outlying galaxies would have been even more tenuous (Tully 1982).

A small number of our associations are special cases. Close to some of the major clusters, there are entities that would be called groups if the major cluster is ignored but that are shown to be disrupted when the influence of the cluster is considered. These entities are suspected to be falling into the clusters. The most apparent case was discussed by Tully and Shaya (1984): association $11+2+1$ near the Virgo Cluster. Another example is association $41+2+1$ near the Fornax cluster.

It is more difficult to provide a rigorous definition of an association than of a group because of the evident importance of tidal effects at the densities of associations. We do require that densities be in excess of $\rho_a = 2.5 \times 10^8\ L_\odot\ \mathrm{Mpc}^{-3}$, a limit one order of magnitude below the limiting density for the delineation of a group. However, in crowded regions tidal effects cause subcomponent linkages to cut off well above this threshold. In these situations, linkages can be quite different with alternative assumptions about the relationship between the distributions of mass and light.

In our terminology, galaxies can be "associated" on two levels. On the first level, entities are identified that fail the density criterion to be called a group, or that are tidally disrupted, but that pass the density criterion to be called an association. At a second level, several groups or first level associations or individual galaxies may link together at densities that satisfy the definition of an association.

According to our nomenclature, a galaxy is assigned to structure identified by three two-digit numbers: $xx \pm yy + zz$. We say that the galaxy is in the xx cloud or spur, the $-yy$ group or $+yy$ first-level association, and the $+zz$ second-level association. If zz is not given, then zz is assumed to be the same as $|yy|$.

g) Clouds and Spurs

In the NBG atlas, it is shown that the local region is laced with a network of connected filaments. Names are given to the major features. Identifications with these features are incorporated in our group specifications.

In the vast majority of cases, it is easy to assign cloud affiliations because the volume filling factors of clouds are small and they are surrounded by voids. However, clouds are usually connected with other clouds, and there can be some arbitrariness about the actual delineation of where one cloud ends and another begins.

Spurs are like clouds but sparsely populated and closely linked to clouds. If a filamentary structure bifurcates, the less prominent feature might be called a spur. There is a tendency to identify spurs nearby that would not warrant distinction at greater distances.

It is possible to be more precise about the qualification for cloud or spur membership. Initially, assignments were made qualitatively. Afterward, the most tenuously linked galaxies in clouds and those galaxies not identified with any cloud were reconsidered and a rigorous criterion was adopted. A galaxy is linked with a cloud if it is within $6h_{75}{}^{-1}$ Mpc of a high-probability member of the cloud and called isolated if it is farther than $6h_{75}{}^{-1}$ Mpc from any such member ($h_{75} = H_0/75$).

h) Further Comments Regarding Terminology

1. There are galaxies identified with clouds that are not associated with any substructure. Such a system in cloud xx would have the group assignment $xx-0$.

2. Groups and associations within a cloud are numbered in order according to their proximity to the predominant structure within the cloud.

3. The first digit in the cloud name specifies one of seven general regions identified in the NBG atlas. The second digit identifies a specific cloud within the general region.

4. If a galaxy in the general region x cannot be associated with any cloud, then it has the group assignment $x0 \pm yy$ (where $yy = -0$ if the galaxy is not in a group or association).

Our scheme for the specification of associations can break down in one special circumstance. There can be galaxies near to the principal clusters that are identified with a cloud other than the one the cluster lies in. These galaxies might link to the cluster tightly enough to be called associates of the cluster, but our nomenclature does not accommodate the linkage of a galaxy in one cloud with a cluster in another cloud. This situation only arises in close proximity to the Virgo, Ursa Major, and Fornax clusters.

In Appendix B, there is an application of the group-finding techniques described in this paper to the Leo region of the sky and a comparison with other group catalogs. Figure 13 in that appendix illustrates how the region can be decomposed into clouds, associations, and groups.

IV. RESULTS

a) An Overview

In the sample of 2367 galaxies, there are 366 groups of two or more members involving 1525 galaxies (64% of the sample). A further 508 systems (21%) lie in associations, 303 systems (13%) lie outside of groups and associations but are still identified with clouds, and 31 systems (1%) are not identified with any higher order structure.

It was pointed out in Fisher and Tully (1981) that incompletion becomes a significant factor beyond $V_0 = 1500\ \mathrm{km\ s}^{-1}$ with our H I sample because candidates of small angular size had to fulfill a distance estimation criterion based essentially on a luminosity classification and, moreover, the H I detectability of galaxies of a given size decreases with distance. It is evident in a comparison with the results by GH that there are

many galaxies missing from our sample at velocities above 2000 km s^{-1}. Also, our group identifications must be unreliable in the vicinity of the 3000 km s^{-1} cutoff of our sample since some groups must span the cutoff in velocity.

For these reasons, the following analysis only considers those groups within a mean group distance of $25h_{75}^{-1}$ Mpc (distance modulus 32.0 with $H_0 = 75$ km s^{-1} Mpc^{-1}). This distance limit corresponds approximately to $V_0 = 1900$ km s^{-1}, although not exactly because distances are derived using a Virgocentric retardation model. Completion to $B_T^{b,i} = 12.0$ assures completion to $M_B^{b,i} = -20.0$, somewhat fainter than M^*, which was determined for our sample to be -20.18.

Within this restricted volume there are 1427 galaxies, including 991 systems (69%) in 179 groups, 291 systems (20%) in associations, 140 systems (10%) not in groups or associations but still in clouds, and 7 systems (0.5%) not linked with any others. Since it turns out that larger galaxies cluster more strongly than smaller galaxies, the 69% of the galaxies in groups have 77% of the total light.

Although seven galaxies are identified as isolated (farther than $6h_{75}^{-1}$ Mpc from a legitimate member of a cloud), six of these are at low galactic latitude. Hence, our single reasonable isolated galaxy candidate within $25h_{75}^{-1}$ Mpc is $2059-17$ = IC 5078, and even it only barely misses membership in either the Telescopium-Grus Cloud (nearest neighbor at $6.1h_{75}^{-1}$ Mpc) or the Sagittarius Cloud (nearest neighbor at $6.2h_{75}^{-1}$ Mpc). As a measure of the isolation of this system, the characteristic separation between galaxies in the distance interval $18–25h_{75}^{-1}$ Mpc (IC 5078 is at $20h_{75}^{-1}$ Mpc) if there were a random distribution is (volume/sample size)$^{1/3} = 3.6h_{75}^{-1}$ Mpc. Hence, IC 5078 is only 1.6 times this characteristic separation from its nearest known neighbor. It remains to be demonstrated that there are *any* truly isolated galaxies.

Figure 1 illustrates a property of the sample that is akin to a multiplicity function. Along the abscissa is the number of members within a group, N_g, and up the ordinate is the cumulative percentage of galaxies in groups with $\leq N_g$ members. Thirty percent of the sample is accounted for by the 438 singles (including associated galaxies). Then approximately 10% of the sample is in each of the following increments: (1) the 78 pairs, (2) the 36 triples, (3) the 32 groups of four to six members, (4) the 17 groups of seven to 11, (5) the 10 groups of 12 to 19, (6) the five groups of 20–60, and (7) the Virgo Cluster.

The actual group assignments for individual galaxies are recorded in the NBG catalog and there is a cross-reference table in that catalog that lists the membership of each group, association, and cloud. Table 2, in this paper, provides a summary of the properties of the 336 groups. Table 3 in Appendix A provides correspondence with other group catalogs.

b) The Groups Have Probably Collapsed

Ideally, we have defined groups with the optimal choice of density such that all our groups have collapsed but less dense structures have not had time to do so. The apparent core-halo nature of groups provided some guidance as to the choice of the optimal density because it might be supposed that cores have collapsed and halos have not. In any event, having selected a specific density for the delineation of groups, it is possible to test the hypothesis that the proposed groups are bound and have collapsed. We offer three tests.

Test 1 involves the standard crossing time argument. The characteristic crossing time is:

$$t_x = \frac{1.5^{1/2} R_I}{3^{1/2} V_p}, \tag{3}$$

where R_I is the inertial radius defined by Jackson (1975) and V_p

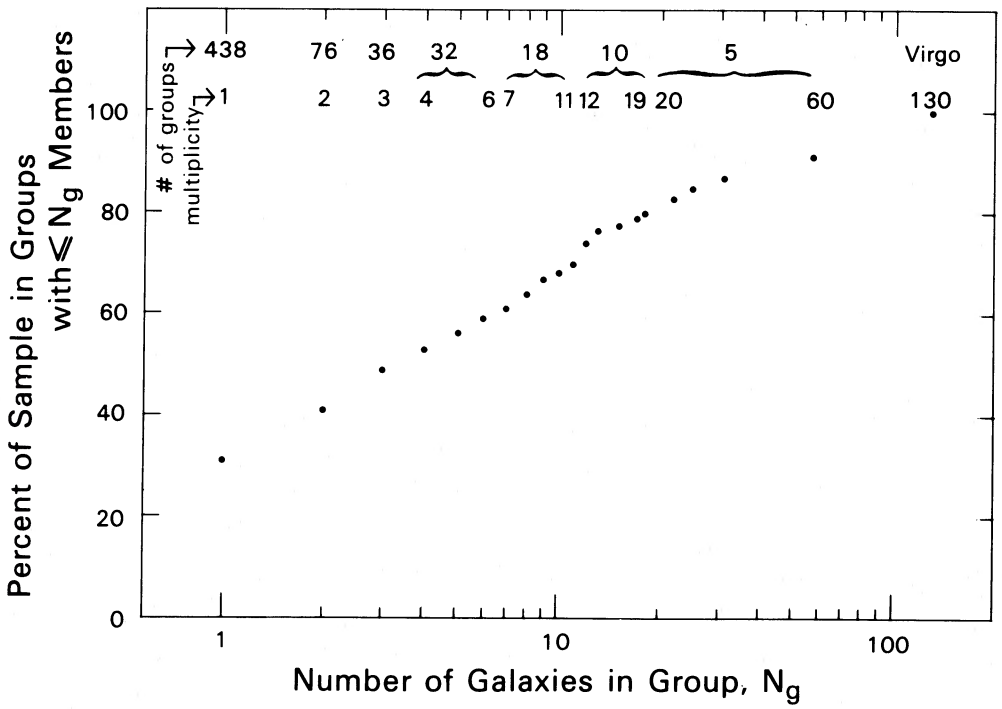

FIG. 1.—Spectrum of group sizes. The percentage of galaxies that are part of groups with memberships $\leq N_g$ are plotted as a function of membership N_g. Thirty percent of the sample are singles, and roughly 10% are in each of the seven other membership intervals identified along the top of the figure.

TABLE 2

GROUP PROPERTIES

	Group	No.	log L_B	V_b	Dist.	V_p	σ_v	R_I	R_v	T_xH_0	T_cH_0	M/L
Virgo Cluster and Southern Extension												
*	11 -1	130	12.20	1042.	16.8	715.	6.	1.02	0.79	0.08	0.20	562.
+	11 -3	2	9.87	1920.	15.3	0.	0.	0.04	0.06	...	...	...
*	11 -4	7	10.59	1576.	13.8	124.	7.	0.30	0.18	0.13	0.26	151.
+	11 -5	2	10.28	1077.	24.2	108.	29.	0.22	0.39	0.11	0.64	514.
+	11 -8	2	10.25	1484.	14.2	110.	22.	0.10	0.19	0.05	0.30	273.
*	11-10	9	11.36	1221.	23.9	79.	6.	0.54	0.44	0.36	1.02	27.
	11-11	8	11.35	1307.	25.4	86.	12.	0.45	0.48	0.28	1.01	34.
+	11-12	3	10.67	1007.	21.3	34.	5.	0.26	0.18	0.41	0.99	10.
+	11-13	2	9.73	1291.	24.2	194.	4.	0.08	0.13	0.02	0.12	2008.
*	11-14	5	11.50	838.	19.2	106.	6.	1.10	0.66	0.55	1.12	51.
+	11-15	2	10.43	1154.	22.0	77.	22.	0.19	0.29	0.13	0.69	139.
	11-17	5	10.98	1504.	27.2	106.	9.	0.45	0.53	0.23	0.90	137.
+	11-18	2	10.99	1282.	23.1	91.	5.	0.40	0.80	0.23	1.58	150.
+	11-19	2	10.38	1270.	22.6	83.	7.	0.20	0.35	0.13	0.77	218.
	11-20	2	11.00	1659.	28.1	76.	28.	0.14	0.25	0.09	0.60	31.
	11-21	5	11.13	1569.	26.5	190.	22.	0.52	0.70	0.15	0.67	406.
	11-22	5	11.30	1754.	28.4	87.	10.	0.82	0.94	0.51	1.97	77.
	11-23	2	10.54	2044.	31.9	29.	7.	0.09	0.19	0.17	1.16	10.
	11-24	12	11.74	2148.	35.2	311.	17.	0.69	0.48	0.12	0.28	184.
	11-25	2	10.45	1970.	33.0	55.	8.	0.14	0.22	0.13	0.72	51.
	11-27	3	11.15	2203.	35.1	68.	21.	0.63	0.95	0.49	2.56	67.
	11-28	2	10.64	2272.	35.6	106.	10.	0.23	0.44	0.12	0.75	247.
	11-29	2	11.49	2489.	38.6	0.	0.	0.11	0.21	...	...	...
	11-30	3	11.35	2483.	38.3	74.	24.	0.32	0.43	0.23	1.06	23.
	11-31	4	11.26	2467.	37.8	94.	28.	0.38	0.32	0.22	0.62	34.
	11-32	2	11.12	2183.	33.2	0.	0.	0.50	0.97	...	...	...
	11-33	4	11.23	2644.	39.6	147.	8.	0.47	0.37	0.17	0.45	100.
	11-34	2	11.31	2815.	42.6	51.	32.	0.04	0.08	0.04	0.29	2.
	11-35	3	11.32	2484.	37.0	44.	13.	0.69	0.95	0.84	3.95	19.
Ursa Major Cloud												
*	12 -1	57	11.70	967.	17.2	148.	6.	1.30	0.98	0.47	1.19	95.
+	12 -2	3	10.68	1179.	20.6	152.	3.	0.29	0.31	0.10	0.37	333.
*	12 -3	9	11.01	1352.	22.9	112.	5.	0.71	0.70	0.34	1.13	185.
+	12 -4	2	10.09	1261.	20.9	194.	12.	0.25	0.41	0.07	0.38	2704.
*	12 -5	6	10.95	1384.	23.0	83.	13.	0.61	0.28	0.39	0.62	47.
*	12 -6	9	10.91	1020.	20.1	125.	14.	0.64	0.30	0.27	0.43	126.
+	12 -7	4	10.73	1310.	20.9	142.	10.	0.54	0.44	0.20	0.56	365.
+	12 -8	2	10.13	1329.	21.2	0.	0.	0.28	0.50	...	...	...
	12 -9	2	10.27	1807.	27.9	58.	28.	0.29	0.46	0.27	1.45	180.
+	12-10	4	11.01	1500.	22.8	130.	24.	0.42	0.51	0.17	0.71	181.
+	12-11	3	10.51	1028.	16.0	69.	6.	0.56	0.85	0.43	2.22	278.
	12-12	6	11.37	1887.	29.5	161.	24.	0.46	0.47	0.15	0.53	115.
	12-13	2	10.54	2004.	30.9	143.	26.	0.07	0.13	0.03	0.17	173.
	12-14	2	10.51	2161.	31.8	42.	20.	0.02	0.03	0.03	0.13	4.
	12-16	2	11.19	2499.	37.4	0.	0.	0.42	0.77	...	...	...
	12-17	2	10.49	2351.	33.7	0.	0.	0.08	0.14	...	...	...
	12-18	2	10.97	2945.	43.0	0.	0.	0.24	0.45	...	...	...
+	12-19	3	10.96	1469.	21.0	122.	10.	0.24	0.18	0.10	0.28	66.
	12-20	2	11.74	2011.	27.7	182.	6.	0.12	0.24	0.04	0.24	32.
	12-21	2	10.48	2650.	37.7	122.	20.	0.21	0.33	0.09	0.50	353.
Ursa Major Southern Spur												
+	13 -1	4	10.81	1190.	20.2	26.	46.	0.67	0.28	1.34	1.93	7.
+	13 -2	2	9.53	932.	16.6	7.	23.	0.08	0.14	0.62	3.86	4.
+	13 -3	2	9.72	1381.	23.6	68.	22.	0.13	0.26	0.10	0.69	492.
+	13 -4	2	10.01	982.	16.6	0.	0.	0.08	0.13	...	...	...
	13 -5	5	10.90	1705.	26.2	100.	15.	0.36	0.06	0.19	0.10	16.
+	13 -6	4	11.01	1475.	23.3	37.	100.	0.46	0.44	0.67	2.17	12.
	13 -7	4	10.62	1476.	26.5	86.	24.	0.54	0.66	0.33	1.38	257.
	13 -8	3	11.08	2042.	32.9	0.	0.	0.70	0.90	...	...	...
	13 -9	2	10.69	1695.	29.7	0.	0.	0.15	0.30	...	...	...
	13-10	2	10.46	2387.	37.1	104.	86.	0.19	0.37	0.10	0.64	297.
	13-11	2	10.82	2431.	38.4	0.	0.	0.54	0.91	...	...	...

TABLE 2—*Continued*

	Group	No.	log L_B	V_b	Dist.	V_p	σ_v	R_I	R_V	T_xH_0	T_cH_0	M/L
	Coma - Sculptor Cloud											
*	14 -1	25	11.00	911.	9.7	266.	12.	0.50	0.34	0.10	0.23	523.
+	14 -2	2	10.48	1191.	12.4	0.	0.	0.05	0.08	...	...	...
*	14 -4	22	10.78	596.	7.6	58.	26.	0.62	0.38	0.56	1.19	46.
*	14 -5	8	10.77	571.	7.3	129.	3.	0.46	0.22	0.19	0.31	134.
*	14 -6	5	10.44	698.	7.8	78.	14.	0.29	0.24	0.20	0.56	116.
*	14 -7	22	10.24	309.	3.5	51.	3.	0.39	0.28	0.41	1.00	93.
*	14 -9	9	10.46	367.	5.0	82.	2.	0.33	0.23	0.21	0.51	117.
*	14-10	12	10.46	242.	3.3	108.	3.	0.35	0.20	0.17	0.33	174.
*	14-11	8	11.17	188.	3.0	75.	5.	0.47	0.25	0.33	0.61	20.
*	14-12[a]	10	10.78	-18.	0.0	57.	2.	0.43	0.15	0.40	0.47	17.
*	14-13	11	10.38	197.	2.1	118.	4.	0.43	0.26	0.19	0.40	328.
+	14-14	2	9.72	292.	4.1	51.	5.	0.29	0.49	0.30	1.74	528.
*	14-15	12	10.96	304.	4.3	68.	4.	0.66	0.46	0.52	1.22	50.
+	14-16	3	10.42	324.	5.6	106.	8.	0.45	0.43	0.23	0.74	404.
+	14-17	2	8.89	574.	7.1	0.	0.	0.03	0.04	...	...	...
+	14-18	2	10.16	979.	9.7	34.	3.	0.16	0.29	0.25	1.57	52.
	Leo Spur											
*	15 -1	9	10.62	626.	7.2	112.	9.	0.22	0.14	0.10	0.23	92.
+	15 -2	4	10.61	640.	6.7	97.	4.	0.08	0.08	0.05	0.15	41.
+	15 -3	2	9.70	951.	12.2	0.	0.	0.17	0.26	...	...	...
+	15 -4	3	9.72	629.	7.4	0.	0.	0.08	0.07	...	...	...
+	15 -5	2	9.89	462.	6.4	0.	0.	0.14	0.21	...	...	...
+	15 -6	2	9.81	441.	6.7	94.	7.	0.24	0.36	0.13	0.69	1078.
+	15 -9	3	10.26	779.	11.8	33.	5.	0.44	0.61	0.71	3.38	77.
+	15-10	3	10.14	756.	13.0	0.	0.	0.43	0.54	...	...	...
+	15-11	2	9.70	585.	10.3	11.	5.	0.12	0.22	0.56	3.58	12.
	Centaurus Spur											
+	16 -1	4	10.84	1105.	18.1	133.	8.	0.95	1.23	0.38	1.68	675.
	16 -2	2	10.69	1635.	25.4	79.	4.	0.23	0.46	0.16	1.06	130.
+	16 -3	2	10.59	1609.	24.7	210.	7.	0.29	0.46	0.07	0.40	1137.
+	16 -4	3	10.57	1269.	21.3	7.	129.	0.40	0.48	2.91	11.98	2.
+	16 -5	2	10.50	1130.	19.3	104.	10.	0.43	0.76	0.22	1.31	566.
	Triangulum Spur											
*	17 -1	13	10.78	752.	10.0	36.	3.	0.58	0.53	0.85	2.66	25.
+	17 -2	2	10.14	879.	11.9	0.	0.	0.45	0.76	...	...	...
+	17 -3	3	9.86	1151.	14.8	24.	4.	0.22	0.32	0.49	2.38	56.
*	17 -4	6	10.57	813.	9.8	114.	4.	0.53	0.35	0.25	0.56	266.
+	17 -5	2	9.79	549.	7.0	57.	7.	0.02	0.02	0.02	0.06	23.
+	17 -7	2	10.28	1167.	13.7	0.	0.	0.21	0.39	...	...	...
	Perseus Cloud											
	18 -1	2	11.49	2602.	34.2	52.	5.	0.85	1.62	0.87	5.65	30.
	18 -2	2	11.31	2889.	37.7	10.	14.	0.36	0.72	1.88	12.80	1.
	Pavo - Ara Spur											
*	19 -1	8	10.86	735.	10.6	87.	6.	0.65	0.35	0.39	0.72	79.
+	19 -2	4	10.70	896.	13.5	134.	7.	0.71	0.94	0.28	1.27	735.
+	19 -3	3	11.02	1364.	19.8	36.	5.	0.60	0.27	0.88	1.38	7.
+	19 -4	2	10.13	805.	10.5	0.	0.	0.24	0.39	...	...	...
+	19 -5	2	9.87	775.	9.6	156.	6.	0.27	0.39	0.09	0.46	2834.
+	19 -6	4	10.42	1030.	12.5	132.	6.	0.29	0.36	0.12	0.50	528.
+	19 -7	4	10.53	680.	8.1	24.	10.	0.37	0.35	0.81	2.60	13.
+	19 -8	2	9.61	553.	6.3	58.	4.	0.11	0.22	0.10	0.69	400.

is the probable velocity dispersion; that is, the observed velocity dispersion corrected for measurement errors (Materne 1974; the corrections are almost always very small with our sample). No luminosity weights are applied. The numerical factors are statistical adjustments to three dimensions. The distance scale independent parameter t_xH_0 is recorded in Table 2 and a histogram of the values of this parameter for the 179 groups within $25h_{75}^{-1}$ Mpc is given in Figure 2. The filled histogram emphasizes the most reliable data: that associated with the 49 groups with at least five members. For this best data, the median value of t_xH_0 is 0.3 and essentially all values of t_x are less than a Hubble time.

Test 2 is a collapse time scale argument. The collapse time is (adapted from Gunn and Gott 1972):

$$t_c = 8.5 \times 10^6 (R_V^3/M_V)^{1/2} \quad (4)$$

in years, where R_V is the virial radius in Mpc (related to a harmonic radius; see footnote 2) and M_V is the virial mass in

TABLE 2—*Continued*

	Group	No.	log L_B	V_b	Dist.	V_p	σ_v	R_I	R_v	T_xH_0	T_cH_0	M/L
	Leo Cloud											
*	21 -1	11	11.28	1087.	22.9	220.	18.	0.61	0.30	0.15	0.25	165.
+	21 -2	3	10.04	1133.	23.0	100.	6.	0.41	0.57	0.22	1.03	1131.
*	21 -3	10	10.82	1009.	20.9	98.	16.	0.51	0.23	0.28	0.43	75.
+	21 -4	2	10.34	893.	16.9	0.	0.	0.17	0.28	...	...	...
+	21 -5	3	10.83	1150.	22.6	9.	27.	0.46	0.68	2.64	13.17	2.
*	21 -6	12	11.15	1207.	22.3	124.	22.	0.86	0.30	0.37	0.44	71.
	21 -7	2	10.60	1408.	25.8	95.	10.	0.05	0.08	0.03	0.15	39.
+	21 -8	4	10.80	1296.	23.5	72.	22.	0.28	0.20	0.20	0.51	37.
	21 -9	4	10.94	1623.	27.7	67.	18.	0.26	0.09	0.20	0.25	10.
*	21-10	5	10.77	1082.	20.1	61.	24.	0.57	0.20	0.49	0.58	27.
	21-11	5	10.94	1343.	25.7	129.	14.	0.39	0.39	0.16	0.55	159.
*	21-12	10	11.02	1453.	24.5	88.	20.	0.65	0.38	0.39	0.78	62.
+	21-13	2	10.33	1435.	24.4	0.	0.	0.16	0.31	...	...	...
+	21-14	2	9.98	1456.	24.5	132.	7.	0.15	0.31	0.06	0.42	1207.
	21-15	2	10.55	1597.	25.9	51.	9.	0.44	0.71	0.46	2.53	112.
	21-16	2	10.38	1725.	27.2	0.	0.	0.02	0.02	...	...	...
	21-17	3	10.30	1716.	27.1	202.	28.	0.06	0.05	0.02	0.04	207.
	21-18	5	11.00	1993.	30.6	122.	10.	0.70	0.34	0.31	0.50	110.
	Crater Cloud											
	22 -1	13	11.55	1491.	25.9	99.	19.	1.00	0.59	0.54	1.07	35.
	22 -2	3	10.58	1536.	27.2	0.	0.	0.43	0.63	...	...	...
+	22 -3	2	9.38	1042.	21.3	75.	10.	0.05	0.09	0.03	0.23	485.
	22 -4	9	11.39	1591.	26.3	121.	17.	0.93	0.71	0.41	1.07	91.
	22 -5	3	11.10	1835.	29.2	155.	12.	0.19	0.05	0.07	0.06	22.
+	22 -6	2	10.74	1238.	21.5	0.	0.	0.41	0.71	...	...	...
	22 -7	3	10.99	1606.	27.8	45.	48.	0.71	0.92	0.84	3.71	42.
	22 -8	2	10.22	1416.	26.2	127.	22.	0.09	0.15	0.04	0.21	320.
	22 -9	2	10.41	1479.	27.3	0.	0.	0.13	0.21	...	...	...
	22-10	2	10.51	1311.	25.9	0.	0.	0.31	0.49	...	...	...
	22-11	2	10.64	1192.	25.2	0.	0.	0.05	0.11	...	...	...
	Centaurus Cloud											
	23 -1[b]	12	...	...	46.3	...	...	...	...	...	...	...
	23 -2	2	11.23	2687.	38.6	60.	32.	0.23	0.44	0.21	1.33	20.
	23 -3	3	11.43	2736.	39.1	114.	16.	0.44	0.52	0.20	0.83	56.
	23 -4	2	10.95	2600.	37.3	55.	32.	0.34	0.64	0.33	2.11	47.
	23 -5	3	11.28	2442.	36.5	39.	14.	0.74	1.08	1.02	5.08	18.
	23 -6	2	11.16	2683.	38.4	39.	36.	0.45	0.76	0.61	3.48	18.
	23 -7	2	10.88	1966.	29.7	0.	0.	0.37	0.58	...	...	...
	23 -8	2	10.96	1960.	29.2	75.	29.	0.09	0.18	0.07	0.45	24.
+	23 -9	2	10.95	1132.	18.5	0.	0.	0.21	0.42	...	...	...
	Lynx Cloud											
	24 -1	4	11.11	2129.	30.4	123.	6.	0.44	0.54	0.19	0.80	140.
+	24 -2	2	10.12	1510.	22.6	48.	4.	0.43	0.68	0.47	2.57	262.
+	24 -3	2	10.21	1600.	24.3	0.	0.	0.03	0.04	...	...	...
	Antlia - Hydra Cloud											
	31 -1[b]	2	...	...	48.5	...	...	...	...	...	...	...
	31 -2	7	11.12	2188.	37.5	479.	30.	0.13	0.11	0.01	0.04	434.
	31 -3	2	11.14	2636.	38.5	0.	0.	0.06	0.11	...	...	...
	31 -4	5	11.54	2517.	36.6	141.	18.	0.81	0.60	0.31	0.77	75.
	31 -5	4	11.40	2334.	34.6	149.	15.	0.71	0.94	0.25	1.14	178.
	31 -6	3	11.81	2647.	38.1	52.	31.	0.97	0.53	1.00	1.87	5.
	31 -7	2	11.19	2556.	37.2	0.	0.	0.18	0.31	...	...	...
	31 -8	3	11.33	2343.	33.8	123.	11.	0.66	1.07	0.28	1.58	166.
	31-10	4	11.60	2555.	37.4	285.	24.	0.09	0.11	0.02	0.07	49.
	31-11	2	11.18	2745.	40.1	0.	0.	0.15	0.25	...	...	...
	31-12	4	11.34	2009.	30.5	168.	34.	0.59	0.78	0.19	0.84	217.
	31-13	2	10.42	1839.	28.5	0.	0.	0.10	0.19	...	...	...
	31-14	3	10.67	1740.	27.0	81.	12.	0.28	0.24	0.18	0.53	75.
	31-15	2	10.79	1968.	30.5	0.	0.	0.02	0.02	...	...	...
	31-16	3	10.38	1675.	26.4	14.	15.	0.19	0.24	0.71	3.06	4.
	31-18	3	10.75	1776.	28.4	22.	22.	0.61	0.56	1.51	4.72	10.
	31-19	3	10.41	1646.	27.0	45.	7.	0.32	0.47	0.38	1.90	79.
	31-20	2	10.10	1726.	28.1	40.	6.	0.16	0.29	0.22	1.32	79.
+	31-21	3	11.66	1348.	20.6	23.	55.	0.88	1.00	2.03	7.82	3.
+	31-22	2	10.83	1461.	22.6	63.	12.	0.28	0.44	0.24	1.28	56.
+	31-23	2	10.30	1053.	18.2	110.	21.	0.27	0.40	0.13	0.65	522.
+	31-24	2	9.61	1051.	16.8	7.	38.	0.24	0.46	1.86	12.32	11.

TABLE 2—*Continued*

	Group	No.	log L_B	V_b	Dist.	V_p	σ_v	R_I	R_v	T_xH_0	T_cH_0	M/L
	Cancer - Leo Cloud											
	32 -1	3	10.95	2609.	38.4	0.	0.	0.38	0.06	...	...	...
	32 -4	2	11.30	2904.	43.6	0.	0.	0.52	0.90	...	...	...
	Carina Cloud											
	33 -1	2	10.79	2526.	35.0	0.	0.	0.36	0.70	...	...	...
	33 -2	2	11.10	2661.	36.8	24.	33.	0.10	0.20	0.22	1.51	2.
	33 -3	2	10.87	1875.	26.8	52.	13.	0.61	1.13	0.62	3.93	91.
	33 -4	2	11.24	2906.	39.3	0.	0.	0.18	0.32	...	...	...
	Lepus Cloud											
+	34 -1	3	10.52	1473.	20.6	93.	9.	0.30	0.39	0.17	0.77	226.
+	34 -2	2	10.49	1506.	20.5	32.	7.	0.50	0.79	0.82	4.43	59.
+	34 -3	3	10.70	1828.	24.1	58.	4.	0.35	0.51	0.32	1.58	75.
	34 -4	2	10.58	2241.	29.6	113.	6.	0.02	0.02	0.01	0.03	15.
	34 -6	2	10.73	1883.	25.9	163.	8.	0.52	1.01	0.17	1.13	1097.
	34 -8	3	11.44	2502.	33.7	0.	0.	1.01	1.50	...	...	...
	Virgo - Libra Cloud											
	41 -1	11	11.51	1807.	28.4	344.	11.	0.49	0.27	0.08	0.14	214.
	41 -2	14	11.61	1701.	28.3	136.	23.	1.25	0.86	0.49	1.15	85.
	41 -3	8	11.28	1611.	27.7	120.	14.	0.78	0.21	0.34	0.31	34.
	41 -4	3	10.67	1563.	27.2	95.	28.	0.47	0.66	0.26	1.26	281.
	41 -5	2	10.85	2225.	34.9	46.	12.	0.02	0.02	0.02	0.08	1.
	41 -6	2	11.02	1895.	29.8	102.	8.	0.50	1.00	0.26	1.78	213.
*	41 -7	5	11.07	1219.	24.0	132.	23.	0.39	0.19	0.16	0.26	61.
+	41 -8	3	10.77	1079.	22.4	62.	8.	0.28	0.32	0.23	0.93	45.
	41-10	3	11.32	2172.	33.0	90.	20.	0.76	1.08	0.45	2.16	91.
	41-11	3	11.12	2302.	34.3	114.	36.	0.03	0.04	0.01	0.07	9.
	41-12	2	11.13	2390.	37.0	108.	30.	0.02	0.02	0.01	0.03	4.
	41-13	2	11.30	2659.	40.2	132.	25.	0.46	0.90	0.18	1.24	171.
	41-14	2	11.24	2571.	38.5	0.	0.	0.02	0.04	...	...	...
	Canes Venatici - Camelopardalis Cloud											
	42 -1	15	11.97	2478.	37.8	162.	12.	1.14	0.59	0.37	0.66	36.
	42 -2	4	11.01	2556.	38.6	16.	33.	0.41	0.22	1.37	2.55	1.
	42 -3	6	11.45	2395.	36.1	73.	7.	0.76	0.44	0.56	1.10	18.
	42 -4	4	11.06	2135.	33.0	139.	22.	0.52	0.14	0.20	0.19	52.
	42 -5	2	10.65	2546.	37.7	65.	8.	0.47	0.85	0.38	2.36	178.
	42 -6	4	10.97	2045.	31.6	111.	18.	0.62	0.49	0.29	0.81	144.
	42 -7	3	11.05	2211.	33.3	149.	21.	0.74	1.05	0.26	1.27	456.
	42 -8	6	11.35	2194.	33.2	73.	22.	0.81	0.74	0.59	1.85	39.
	42-12	2	10.13	2316.	34.2	0.	0.	0.04	0.08	...	...	...
	42-13	8	11.29	1905.	28.6	124.	15.	0.71	0.43	0.31	0.63	73.
	42-14	2	11.27	2777.	40.0	0.	0.	0.47	0.74	...	...	...
	42-16	4	11.37	2391.	33.8	184.	14.	0.40	0.24	0.11	0.24	77.
	42-17	2	11.38	2306.	32.8	111.	9.	0.11	0.19	0.05	0.32	22.
	42-18	2	11.20	2672.	36.8	0.	0.	0.49	0.87	...	...	...
	42-19	2	11.79	2745.	37.6	6.	43.	1.07	1.90	9.61	58.28	0.
	Canes Venatici Spur											
*	43 -1	13	11.15	970.	19.2	128.	9.	0.75	0.49	0.31	0.70	124.
+	43 -2	4	10.19	1333.	24.0	38.	13.	0.62	0.62	0.87	2.98	125.
+	43 -3	2	9.54	1342.	23.4	31.	6.	0.02	0.03	0.03	0.18	19.
	Draco Cloud											
*	44 -1	7	10.79	922.	15.9	76.	7.	0.50	0.40	0.35	0.96	83.
+	44 -2	2	10.28	1074.	17.9	34.	4.	0.21	0.31	0.32	1.66	42.
+	44 -3	2	9.21	709.	11.9	36.	4.	0.12	0.22	0.18	1.11	377.
+	44 -4	2	10.20	1086.	17.9	52.	5.	0.39	0.73	0.40	2.56	270.
+	44 -5	2	10.49	1428.	21.8	9.	9.	0.34	0.67	2.01	13.50	4.
+	44 -6	2	10.34	1445.	22.2	112.	7.	0.09	0.17	0.04	0.27	212.
+	44 -7	2	10.26	1527.	23.0	64.	4.	0.26	0.43	0.21	1.23	211.
	44 -8	4	10.94	1854.	26.9	137.	21.	0.79	0.88	0.30	1.16	419.
	Coma Cloud											
	45 -1	3	10.96	2611.	40.3	0.	0.	0.41	0.40	...	...	...

TABLE 2—*Continued*

	Group	No.	log L_B	V_b	Dist.	V_p	σ_v	R_I	R_v	T_xH_0	T_cH_0	M/L
	Fornax Cluster and Eridanus Cloud											
*	51 -1	31	11.48	1344.	16.9	434.	18.	0.56	0.32	0.07	0.13	431.
+	51 -3	3	10.62	1301.	15.9	103.	7.	0.49	0.53	0.25	0.93	298.
*	51 -4	17	11.18	1427.	17.9	110.	13.	0.99	0.50	0.48	0.83	87.
*	51 -5	6	10.87	1601.	19.9	85.	6.	0.53	0.47	0.33	0.99	100.
+	51 -6	2	10.20	1279.	15.8	47.	5.	0.30	0.51	0.34	1.94	156.
*	51 -7	6	10.99	1626.	20.2	112.	10.	0.67	0.23	0.32	0.38	65.
+	51 -8	3	10.78	1653.	20.8	175.	34.	0.28	0.25	0.09	0.26	276.
+	51 -9	2	9.94	1766.	22.5	0.	0.	0.13	0.25	...	...	...
+	51-10	2	9.59	1285.	16.9	0.	0.	0.14	0.26	...	...	...
+	51-11	2	10.87	1993.	25.1	0.	0.	0.58	0.99	...	...	...
+	51-12	3	10.52	1897.	23.7	149.	7.	0.41	0.58	0.15	0.70	843.
	51-13	2	10.42	2214.	27.7	0.	0.	0.18	0.31	...	...	...
	51-14	2	10.86	2576.	32.2	0.	0.	0.16	0.33	...	...	...
	Cetus - Aries Cloud											
*	52 -1	11	10.95	1405.	17.1	99.	4.	0.53	0.44	0.28	0.81	107.
*	52 -2	8	10.91	1125.	13.8	75.	13.	0.64	0.47	0.45	1.14	73.
*	52 -3	5	10.58	1567.	19.1	105.	13.	0.45	0.30	0.23	0.52	190.
+	52 -4	3	10.56	1536.	19.0	8.	8.	0.52	0.67	3.63	15.98	2.
+	52 -5	2	10.31	1416.	17.1	23.	5.	0.22	0.36	0.50	2.86	20.
*	52 -6	6	10.65	1531.	18.6	79.	12.	0.44	0.14	0.29	0.32	43.
*	52 -7	6	11.07	1954.	23.7	48.	6.	0.44	0.36	0.49	1.36	15.
+	52 -8	3	10.40	1890.	22.9	121.	7.	0.15	0.22	0.07	0.32	273.
+	52 -9	4	10.54	1734.	20.9	102.	5.	0.47	0.47	0.24	0.83	306.
+	52-10	2	10.35	1662.	20.4	39.	4.	0.33	0.49	0.45	2.27	71.
+	52-11	2	10.63	1678.	20.4	101.	15.	0.41	0.72	0.22	1.29	374.
	52-12	6	11.36	2416.	29.6	133.	9.	0.85	0.36	0.34	0.50	62.
	52-13	2	10.27	2077.	25.4	6.	7.	0.17	0.30	1.52	8.94	1.
	52-14	3	11.22	2562.	32.1	46.	18.	0.32	0.09	0.37	0.35	3.
	52-15	2	10.97	2851.	35.8	57.	9.	0.38	0.69	0.35	2.18	54.
	Dorado Cloud											
*	53 -1	13	11.04	1006.	13.4	236.	10.	0.34	0.29	0.08	0.22	319.
+	53 -2	3	10.33	1016.	13.6	92.	7.	0.36	0.42	0.21	0.83	370.
*	53 -3	5	10.42	1109.	15.0	121.	6.	0.45	0.38	0.20	0.57	460.
+	53 -4	3	9.96	943.	13.1	143.	14.	0.28	0.44	0.10	0.55	2139.
+	53 -5	2	10.00	1123.	15.1	0.	0.	0.22	0.34	...	...	...
+	53 -6	3	9.39	890.	12.6	51.	9.	0.12	0.17	0.13	0.61	386.
*	53 -7	15	10.75	833.	10.8	93.	7.	0.69	0.48	0.39	0.94	161.
+	53 -8	2	9.81	887.	11.6	0.	0.	0.13	0.25	...	...	...
+	53 -9	2	10.35	741.	9.3	88.	5.	0.15	0.24	0.09	0.49	179.
*	53-10	5	10.51	831.	11.4	103.	7.	0.45	0.25	0.23	0.44	179.
+	53-11	2	9.95	1105.	15.1	33.	5.	0.14	0.24	0.22	1.29	66.
+	53-12	2	9.23	650.	9.0	169.	24.	0.08	0.15	0.03	0.16	5592.
+	53-13	3	10.42	1075.	13.9	73.	31.	0.15	0.05	0.11	0.13	23.
+	53-14	2	9.46	534.	8.1	0.	0.	0.11	0.19	...	...	...
+	53-15	2	10.21	808.	12.5	7.	26.	0.44	0.72	3.58	19.73	4.
+	53-16	2	9.93	706.	11.1	10.	13.	0.26	0.48	1.40	8.65	12.
+	53-17	4	10.69	1149.	16.5	87.	12.	0.52	0.30	0.32	0.62	99.
+	53-18	2	10.23	943.	14.2	63.	7.	0.10	0.18	0.08	0.51	92.
+	53-19	2	10.49	1492.	20.9	0.	0.	0.19	0.29	...	...	...
+	53-20	2	9.55	614.	8.6	31.	7.	0.35	0.53	0.60	3.13	304.
+	53-21	2	10.54	1242.	18.5	206.	16.	0.08	0.14	0.02	0.13	386.
+	53-22	3	10.17	1279.	18.7	130.	12.	0.30	0.49	0.12	0.68	1215.
	Antlia Cloud											
*	54 -1	7	10.72	802.	13.7	111.	8.	0.55	0.42	0.26	0.68	219.
+	54 -2	4	10.53	794.	13.9	63.	17.	0.33	0.41	0.28	1.19	106.
*	54 -3	5	10.28	519.	8.4	68.	17.	0.29	0.31	0.22	0.83	160.
+	54 -5	2	10.46	900.	16.3	62.	6.	0.03	0.05	0.02	0.15	15.
	Apus Cloud											
	55 -1	3	11.13	2846.	38.7	130.	8.	0.50	0.57	0.21	0.80	155.
	55 -2	2	10.75	2526.	34.5	0.	0.	0.25	0.46	...	...	...
	55 -3	2	10.72	2262.	30.3	43.	17.	0.02	0.02	0.02	0.09	2.
	55 -4	2	10.53	2037.	27.6	0.	0.	0.19	0.36	...	...	...
+	55 -5	2	10.30	1741.	23.1	0.	0.	0.28	0.50	...	...	...

TABLE 2—*Continued*

	Group	No.	log L_B	V_b	Dist.	V_p	σ_v	R_I	R_v	T_xH_0	T_cH_0	M/L
	Telescopium - Grus Cloud											
	61 -1	5	11.33	2729.	35.5	133.	33.	0.16	0.16	0.06	0.22	29.
	61 -2	3	11.06	2879.	37.2	98.	18.	0.11	0.17	0.06	0.31	31.
	61 -3	2	10.32	2685.	34.6	0.	0.	0.09	0.17	...	...	...
	61 -4	5	11.15	2683.	35.6	172.	34.	0.23	0.16	0.07	0.17	74.
	61 -5	4	10.91	1900.	25.2	103.	11.	0.47	0.32	0.24	0.56	91.
	61 -6	3	10.90	2482.	31.5	142.	28.	0.55	0.84	0.21	1.08	468.
	61 -7	2	10.74	2925.	37.1	0.	0.	0.10	0.15	...	...	...
	61 -9	3	10.64	2305.	29.1	52.	35.	0.07	0.12	0.07	0.42	16.
	61-10	2	10.72	2022.	25.8	173.	26.	0.10	0.20	0.03	0.21	249.
*	61-11	6	10.71	1852.	23.2	106.	12.	0.45	0.13	0.22	0.23	63.
+	61-12	3	10.74	1898.	24.1	0.	0.	0.33	0.32	...	...	...
+	61-13	2	10.43	1678.	21.5	93.	17.	0.46	0.73	0.26	1.42	507.
	61-15	2	10.17	2117.	26.1	19.	87.	0.18	0.35	0.49	3.29	20.
*	61-16	12	11.25	1572.	19.3	93.	8.	0.84	0.40	0.48	0.78	43.
+	61-17	4	10.70	1536.	18.7	138.	7.	0.21	0.21	0.08	0.28	174.
+	61-18	3	10.73	1562.	18.8	7.	29.	0.53	0.50	3.99	12.87	1.
+	61-19	2	10.31	1520.	18.2	117.	25.	0.22	0.37	0.10	0.58	539.
+	61-20	2	10.41	1588.	19.0	0.	0.	0.46	0.81	...	...	...
+	61-21	3	10.15	1595.	19.0	149.	5.	0.26	0.27	0.09	0.34	935.
+	61-22	2	10.37	1622.	19.4	83.	31.	0.09	0.16	0.06	0.35	101.
+	61-23	3	10.51	1790.	21.5	41.	14.	0.43	0.06	0.55	0.25	7.
+	61-24	2	9.25	1650.	19.7	0.	0.	0.14	0.27	...	...	...
	Pavo - Indus Spur											
	62 -1	2	11.26	2920.	37.7	0.	0.	0.22	0.41	...	...	...
	62 -2	3	10.92	2826.	36.4	75.	31.	0.37	0.41	0.26	0.99	61.
	62 -3	2	10.91	2948.	37.9	0.	0.	0.03	0.06	...	...	...
	Pisces Austrinus Spur											
	63 -1	6	11.12	2657.	33.3	93.	18.	0.55	0.07	0.31	0.14	11.
	63 -2	3	10.78	2681.	33.7	41.	31.	0.41	0.50	0.52	2.20	31.
	63 -3	2	10.34	2690.	33.5	0.	0.	0.06	0.12	...	...	...
	63 -4	2	10.68	2819.	35.3	55.	17.	0.38	0.70	0.37	2.30	97.
+	63 -6	2	10.74	1948.	23.6	0.	0.	0.15	0.29	...	...	...
	Pegasus Cloud											
	64 -1	7	11.08	2349.	29.2	182.	9.	0.46	0.11	0.14	0.11	66.
	64 -2	2	10.99	2698.	33.7	134.	6.	0.71	1.10	0.28	1.49	446.
	64 -3	2	10.14	2124.	26.6	39.	11.	0.03	0.04	0.03	0.16	9.
+	64 -4	3	10.36	1946.	24.1	74.	5.	0.25	0.27	0.18	0.66	143.
+	64 -6	2	10.52	1907.	23.2	114.	19.	0.17	0.34	0.08	0.53	290.
+	64 -7	3	10.23	1979.	24.4	8.	21.	0.29	0.36	1.84	7.81	3.
	64 -8	2	10.94	2577.	32.1	60.	7.	0.31	0.59	0.28	1.79	53.
	64 -9	2	10.99	2773.	34.4	98.	19.	0.02	0.04	0.01	0.07	8.
	64-10	5	11.01	2853.	35.2	98.	11.	0.50	0.15	0.27	0.27	31.
+	64-12	3	10.31	1490.	18.8	161.	9.	0.34	0.35	0.11	0.40	990.
	Pegasus Spur											
*	65 -1	6	10.72	1132.	14.6	74.	5.	0.49	0.42	0.35	1.02	94.
+	65 -2	2	10.29	1494.	18.7	56.	8.	0.02	0.03	0.02	0.10	10.
+	65 -3	3	9.86	1008.	12.5	20.	7.	0.18	0.24	0.47	2.12	29.
+	65 -4	3	10.09	679.	9.0	29.	4.	0.12	0.16	0.23	0.98	23.
+	65 -6	4	10.30	1110.	13.4	90.	15.	0.31	0.36	0.18	0.72	322.
+	65 -7	2	9.24	961.	11.4	91.	78.	0.02	0.02	0.01	0.04	209.
	Sagittarius Cloud											
+	66 -1	2	10.19	1740.	23.1	0.	0.	0.03	0.05	...	...	...

solar units. The distance scale independent parameter $t_c H_0$ is recorded in Table 2 and plotted as a histogram in Figure 3. The median value for the 49 nearby groups with five or more members is $t_c H_0 = 0.6$. For 98% of these groups, $t_c < 2H_0^{-1}$, hence they are collapsing or have already collapsed. Clusters are expected to virialize after roughly $1.5t_c$ through violent relaxation, a condition satisfied by half the groups (the details are slightly dependent on q_0).

Test 3 looks for a signature of an interloper problem. Subsequent to previous attempts to define groups it has usually been found that fainter prospective group members tend to be redshifted with respect to the group mean. The normal interpretation (Byrd and Valtonen 1985 with regard to the HG groups) is that the proposed groups include line-of-sight interlopers, and if they are from the background, then they tend to be fainter. More controversial interpretations invoke non-Doppler redshifts (Arp 1970; Jaakola 1971; Arp and Sulentic 1985). In the top panel of Figure 4 is a histogram of $V_i - V_g$

TABLE 2—*Continued*

Group	No.	log L_B	V_b	Dist.	V_p	σ_v	R_I	R_v	T_xH_0	T_cH_0	M/L
Serpens Cloud											
71 -1	4	11.03	2030.	31.6	118.	10.	0.43	0.09	0.19	0.14	26.
71 -2	2	10.70	1984.	31.0	75.	7.	0.27	0.42	0.19	1.01	102.
71 -3	2	10.36	2291.	34.5	0.	0.	0.27	0.53	...	...	...
71 -4	3	10.95	2065.	31.1	0.	0.	0.42	0.64	...	...	...
71 -5	2	10.35	1975.	30.5	24.	19.	0.07	0.14	0.16	1.06	8.
71 -6	3	10.14	1821.	28.8	0.	0.	0.29	0.30	...	...	...
Boötes Cloud											
72 -1	4	11.19	2686.	39.5	166.	14.	0.38	0.07	0.12	0.08	28.
Ophiuchus Cloud											
73 -1	2	11.04	2494.	34.8	0.	0.	0.28	0.55	...	...	...
73 -1	2	11.04	2494.	34.8	0.	0.	0.28	0.55	...	...	...
73 -2	3	10.77	2052.	29.2	73.	7.	0.25	0.42	0.18	1.05	83.
73 -3	2	10.95	1820.	26.7	17.	5.	0.32	0.51	1.02	5.63	3.
Isolated											
60 -1	2	11.09	2926.	37.9	103.	6.	0.20	0.31	0.10	0.54	58.
70 -1	2	10.18	2179.	32.6	29.	30.	0.02	0.02	0.04	0.13	2.

NOTES.—Group = group identification. No. = number of members. log L_B = logarithm of the sum of the luminosities of group members in $L_\odot$. V_b = barycentric group velocity in km s^{-1}. Dist. = distance from redshift and Virgocentric retardation model in h_{75}^{-1} Mpc. V_p = "probable" velocity dispersion, corrected for observational uncertainties, in km s^{-1}. σ_V = standard error in velocity dispersion in km s^{-1}. R_I = inertial radius in h_{75}^{-1} Mpc. R_V = virial radius in h_{75}^{-1} Mpc. T_xH_0 = crossing time in units of the Hubble time. T_cH_0 = collapse time in units of Hubble time. M/L = virial mass to corrected blue light ratio in solar units. Groups with ≥ five members within $25h_{75}^{-1}$ Mpc are marked with an asterisk. Groups with two to four members within $25h_{75}^{-1}$ Mpc are marked with a plus sign.

[a] Group 14 – 12 (Local Group): Eight Population II systems not included in virial analysis.

[b] Groups 23 – 1 (Centaurus Cluster) and 31 – 1 (Hydra I Cluster) lie outside the survey region, but galaxies with $V_0 < 3000$ km s^{-1} enter our sample.

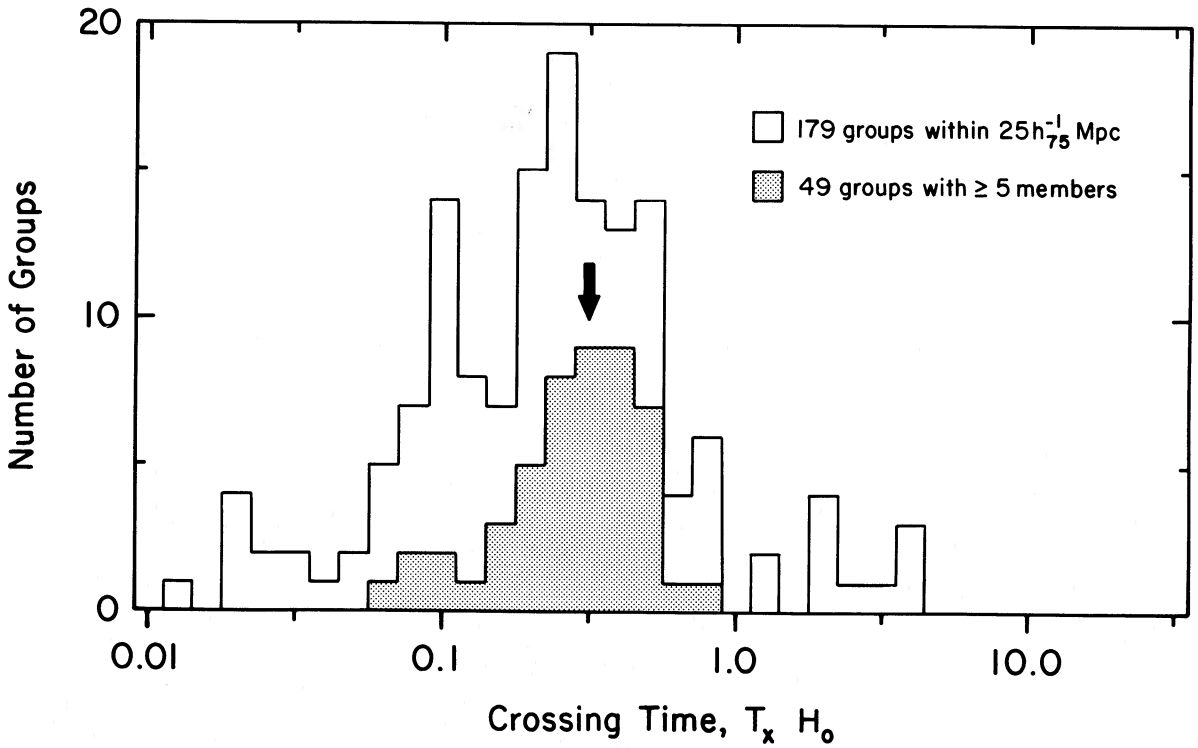

FIG. 2.—Histogram of crossing times. The median value for the 49 large groups within $25h_{75}^{-1}$ Mpc of $t_xH_0 = 0.3$ is indicated by the arrow.

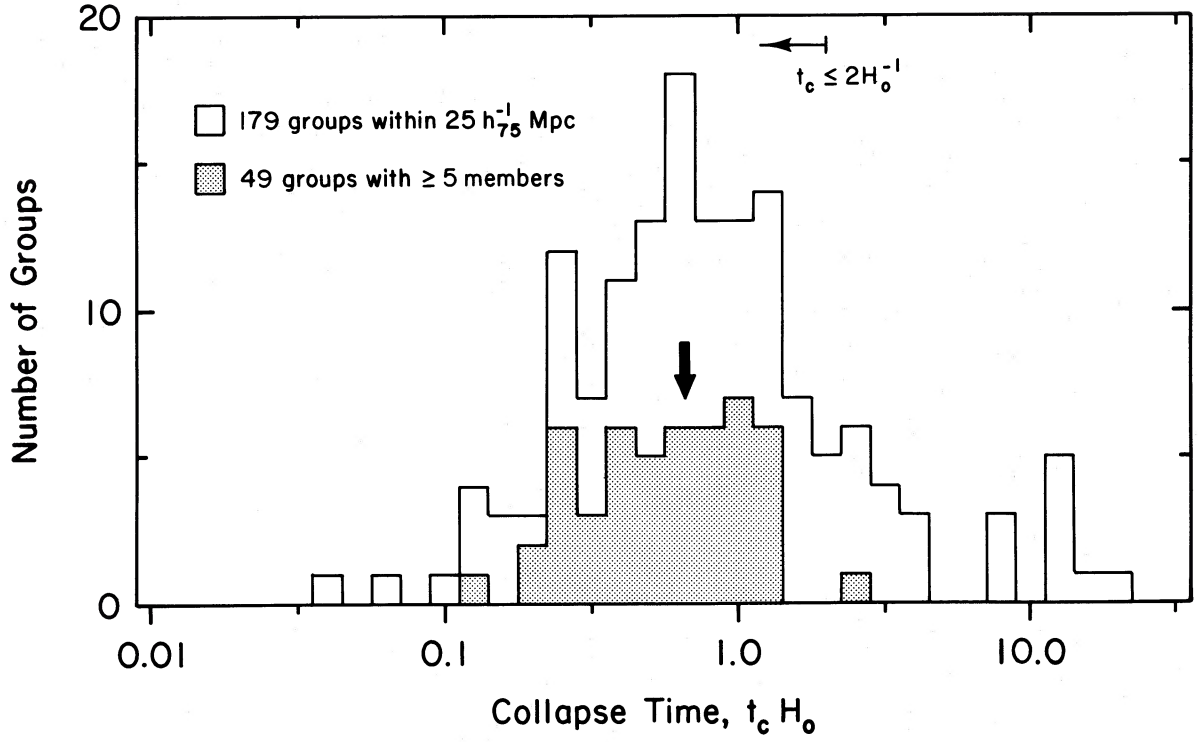

FIG. 3.—Histogram of collapse times. The arrow indicates the median value of $t_c H_0 = 0.6$ for the 49 large, nearby groups. The condition $t_c H_0 < 2$ must be fulfilled if a group has collapsed or is collapsing.

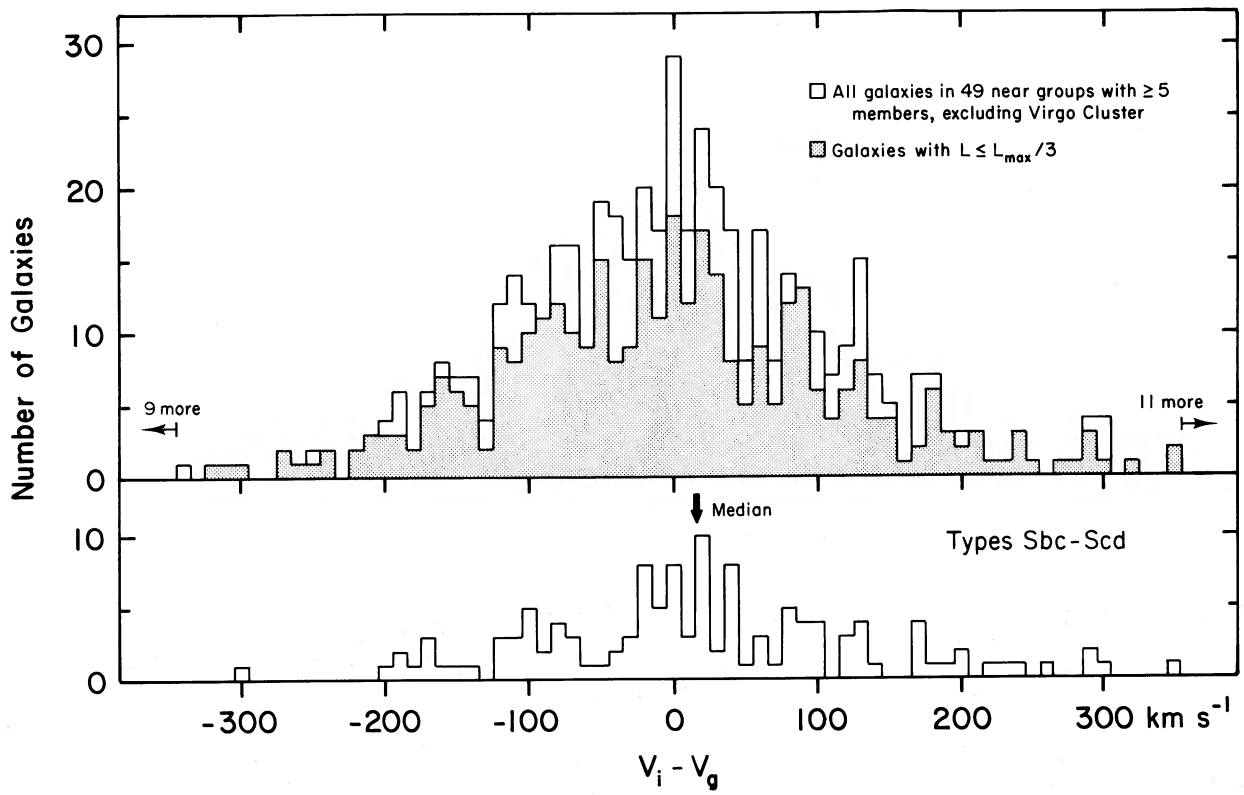

FIG. 4.—Symmetry of the velocities of group members, V_i, with respect to the average group velocity, V_g. The plot in the top panel is a histogram of $V_i - V_g$ values for members of 48 of the 49 nearby groups with at least five members (the Virgo Cluster is excluded). The open histogram includes all members, and the filled histogram includes only members fainter than one-third the luminosity of the brightest galaxy in a group. In the bottom panel is a similar histogram, but it is restricted to types Sbc, Sc, and Scd. The median value is indicated by the arrow and is not significantly displaced from zero.

values for the new group identifications, where the V_i are individual systemic velocities and V_g is the average velocity of the galaxies assigned to the group. The filled histogram involves only those galaxies less luminous than one-third the luminosity of the brightest group member. Evidently, there is not the slightest tendency for faint prospective members to be systematically redshifted. Part of the non-Doppler redshift controversy has involved the contention that Sc galaxies in groups tend to be systematically redshifted. The bottom panel in Figure 4 shows that the effect is not significant with the present catalog.

Positive results on these three tests are necessary but not sufficient evidence that the groups are bound and collapsed. Test 2 leads to a result that is internally consistent. If the virial analysis can be believed, then half the groups collapsed sufficiently long ago that they should, indeed be virialized.

The evidence suggests that we have come close to our intended mark, in that most of our groups have probably collapsed already but, if the threshold density were significantly lowered, then we would begin to include significant numbers of uncollapsed regions. Perhaps half of our groups are reasonably well virialized. There is no evidence of a serious interloper problem, nor of anomalous redshifts.

c) *Group Dimensions*

A histogram of the virial radii of the near 179 groups is given in Figure 5. These results are compared with the HG harmonic

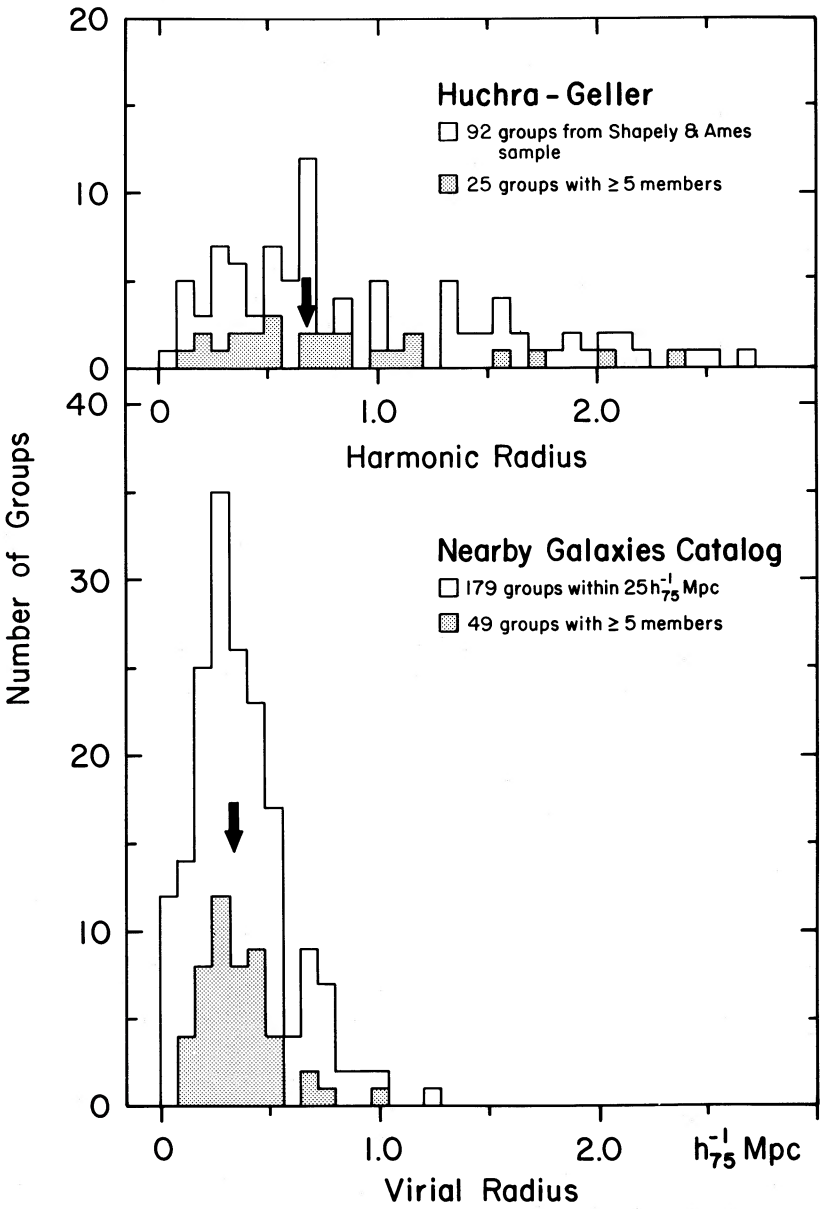

FIG. 5.—Virial radii. The open histogram in the bottom panel illustrates the distribution of R_V values for all groups identified in the NBG catalog within $25h_{75}^{-1}$ Mpc. The filled histogram is for those groups with at least five members and the arrow indicates the median value $\langle R_V \rangle = 340$ kpc for these 49 groups. The equivalent data for the groups found by HG within the Shapley-Ames sample is shown in the top panel (except the abscissa is harmonic radius rather than virial radius; HG data have been adjusted to be consistent with the value of the Hubble constant used here). The arrow indicates the median value of $\langle R_H \rangle = 680$ kpc for the 25 groups with at least five members. HG groups have at least three members, while NBG groups can have as few as two members.

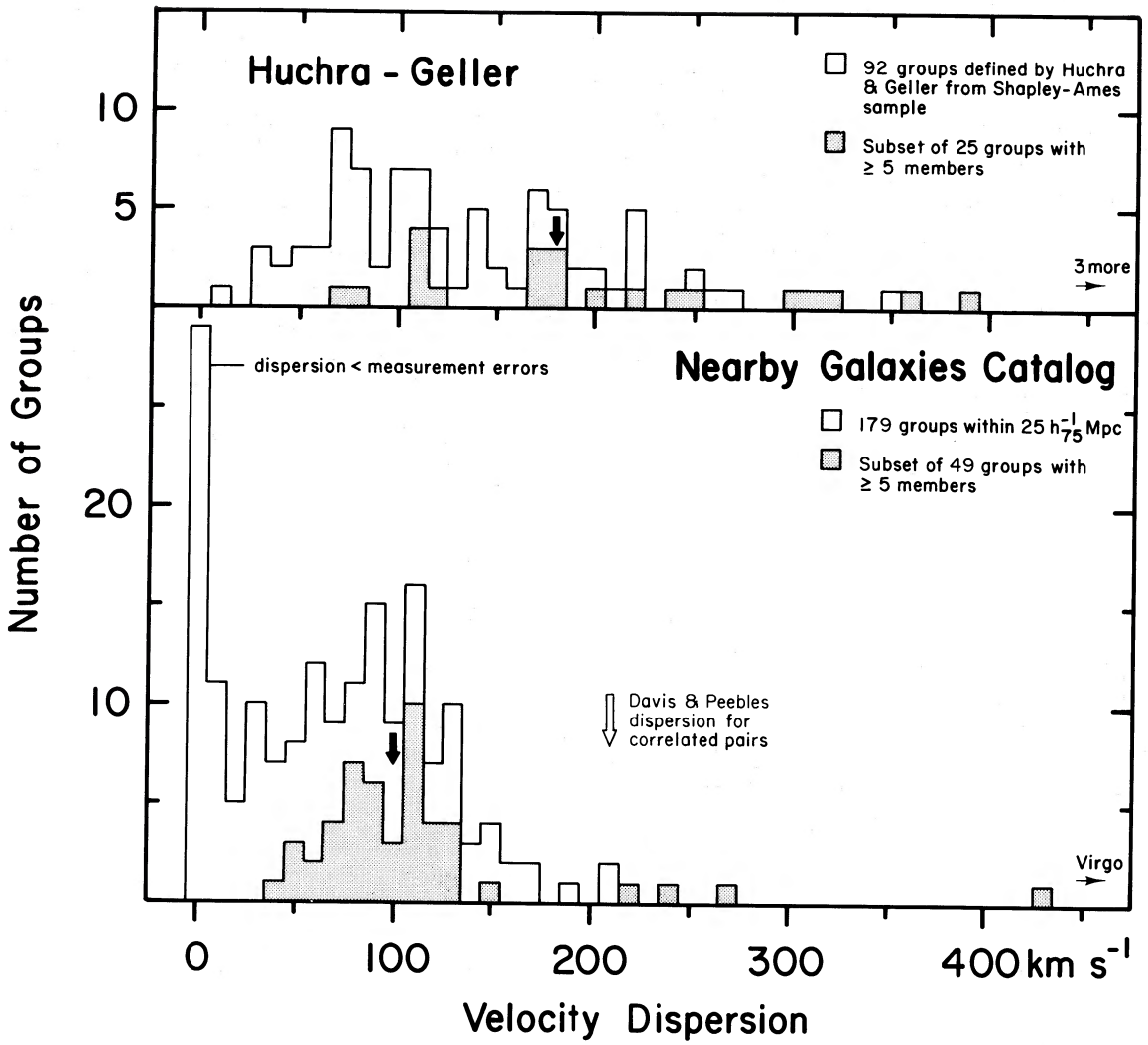

FIG. 6.—Velocity dispersions. In the bottom panel, there are histograms of the rms velocity dispersions for all groups within $25h_{75}^{-1}$ Mpc (*open*) and for those groups with ≥five members (*filled*). The median value of 100 km s^{-1} for the larger groups is indicated by the arrow. The Davis-Peebles correlation dispersion of 210 km s^{-1} at a scale of $300h_{75}^{-1}$ kpc is also indicated. The top panel illustrates the equivalent information for the HG groups found among Shapley-Ames galaxies, and the median dispersion for the larger groups is 180 km s^{-1}.

radii.[2] Evidently, there is a substantial difference between the groups defined in the present analysis and those defined by HG. The median virial radius for our 49 large, nearby groups is $340h_{75}^{-1}$ kpc, with $R_V < 500h_{75}^{-1}$ kpc for 80% of these groups. The median and the dispersion in the dimensions of the HG groups are much larger.

[2] The virial radius, R_V, is defined as

$$R_V = \frac{\sum_{i>j} m_i m_j}{\sum_{i>j} m_i m_j / r_{ij}},$$

while the harmonic radius, R_H, is defined as

$$R_H = \frac{M^2}{\sum_{i \neq j} m_i m_j / r_{ij}}.$$

For equal masses, $R_V/R_H = (n-1)/n$. If masses are unequal, then $R_V/R_H \approx 0.85$ is typical. The parameter R_H is less stable than R_V in cases dominated by a single object. Note that pairs with extremely small values of r_{ij} can dominate the determination of R_V (and nominally possess most of the potential energy of the system). Presumably, extremely small separations are either just projection effects or transient phenomena and should not be given undue weight. We deal with this problem by assuming separations are never less than 20 kpc.

d) Velocity Dispersions

The "probable" velocity dispersions recorded in Table 2 are adjusted for observational uncertainties following Materne (1974). The corrections are almost always small (median correction ≈ 3%), although in 29 groups with four or fewer members the observed dispersion is less than the expected instrumental dispersion. The velocity dispersions are not luminosity weighted.

There is a histogram of the velocity dispersions of the near 179 groups in Figure 6. The median dispersion for the 49 largest groups is 100 km s^{-1}. The most noteworthy feature of the histogram, though, is its asymmetry. Ten percent of the sample lies in a high-velocity tail that extends above 200 km s^{-1} to 715 km s^{-1} (the Virgo Cluster). The histogram for these newly defined groups is also distinctly different from the histogram associated with HG groups. The median dispersion for their 25 largest groups is 180 km s^{-1} and the distribution is much broader.

The open arrow in Figure 6 indicates the one-dimensional velocity dispersion per galaxy between correlated pairs found

by Davis and Peebles (1983: 210 km s^{-1} at separations of $300h_{75}^{-1}$ kpc). This measurement averages over pairwise velocity differences in environments as diverse as moderate clusters and the low-density regions of clouds. Because of the highly nonnormal distribution of the velocity dispersion histogram, the Davis-Peebles value is not characteristic of any important specific clustering constituent.

The Huchra-Geller group dispersions and, probably, the Davis-Peebles correlation dispersions must be elevated because of contamination from interlopers. This point will be raised again in the final section.

e) Mass-to-Light Values

We have calculated the masses of groups in three ways: (1) through the virial theorem with luminosity weighting, (2) through the virial theorem but with no weighting, and (3) through the "projected mass estimator" introduced by Bahcall and Tremaine (1981) and Heisler, Tremaine, and Bahcall (1985). All three methods give consistent results, with a few caveats.

Results from the two virial theorem methods are compared in Figure 7. There is good agreement at large masses, but there is disagreement at low masses in the sense that there is a tail to very low values in the distribution of masses estimated with luminosity weighting. This spurious result arises because in some groups dominated by a few (perhaps only one) massive systems, the velocities of the dominant galaxies determine the luminosity-weighted group barycentric velocity and force the measured velocity dispersion of the group to be artificially low. Moreover, only a small number of luminous systems contribute to the analysis, and large numbers of dwarf "test particles" are virtually ignored. In a circumstance with small numbers, projection effects will produce a spurious low velocity, hence, low-mass tail. Bahcall and Tremaine (1981) have discussed these tendencies, which they characterize as "biases" and "inefficiencies" in luminosity-weighted virial mass estimates.

The unweighted virial analysis and projected mass estimator results are compared in Figure 8. The correlation is seen to be quite tight, and there are no systematic deviations from the anticipated 45° slope. However, the null zero-point offset in Figure 8 was only achieved through adjustment of a poorly constrained normalization factor associated with the projected mass estimator. Bahcall and Tremaine, and Heisler *et al.* prescribe normalization factors, f_{PM}, ranging from $16/\pi$ in the case of a single dominant mass and isotropic orbits to $64/\pi$ in the case of equal masses and radial orbits. The good zero-point agreement in Figure 8 is achieved with the normalization factor $f_{PM} = 20/\pi$. This value of f_{PM} is 33% smaller than the value recommended by Heisler *et al.*, probably because real groups are intermediate in properties between the equal mass and the single dominant mass test cases.

The mass values listed in Table 2 and used in the ensuing analysis are unweighted virial masses. Questions of normalization aside, these masses never differ significantly from the projected mass estimator, which is to say, the differences are small compared with uncertainties due to small number statistics, projection effects, and the nature of the orbits. The unweighted virial mass estimator is considered more reliable than the luminosity weighted virial estimator.

The luminosities in Table 2 are blue luminosities corrected for inclination and galactic obscuration effects following Tully and Fouqué (1985). The mean obscuration correction is 40% in luminosity. Sources for the photometry are given in the

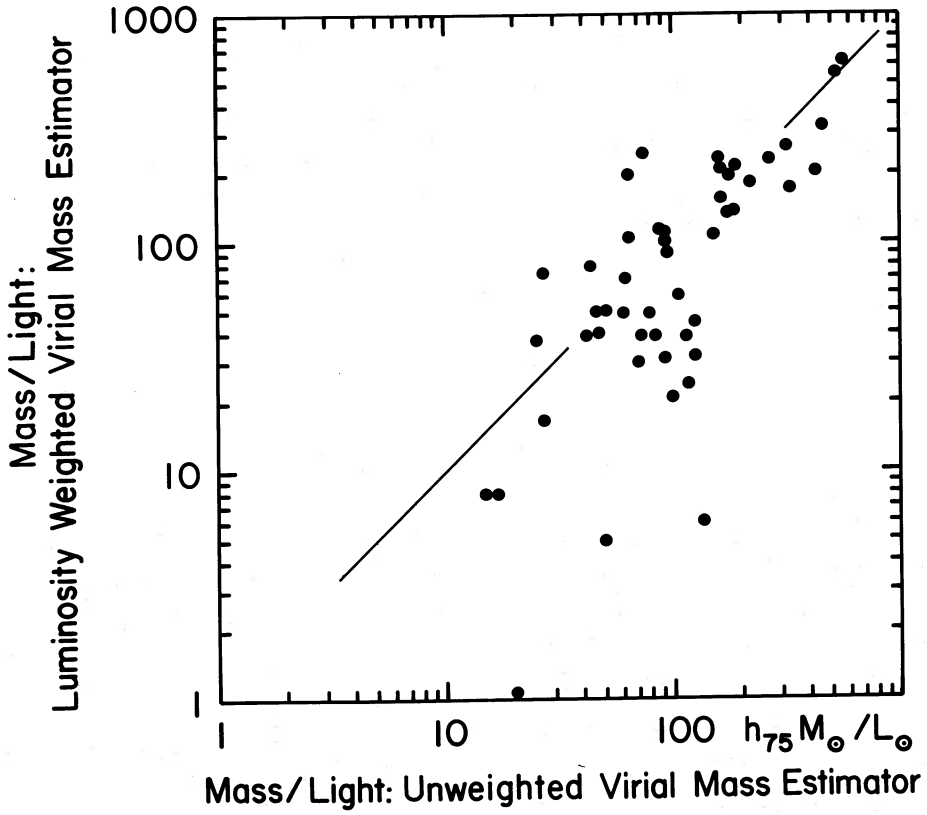

FIG. 7.—Comparison of mass estimators: luminosity weighted vs. unweighted virial masses

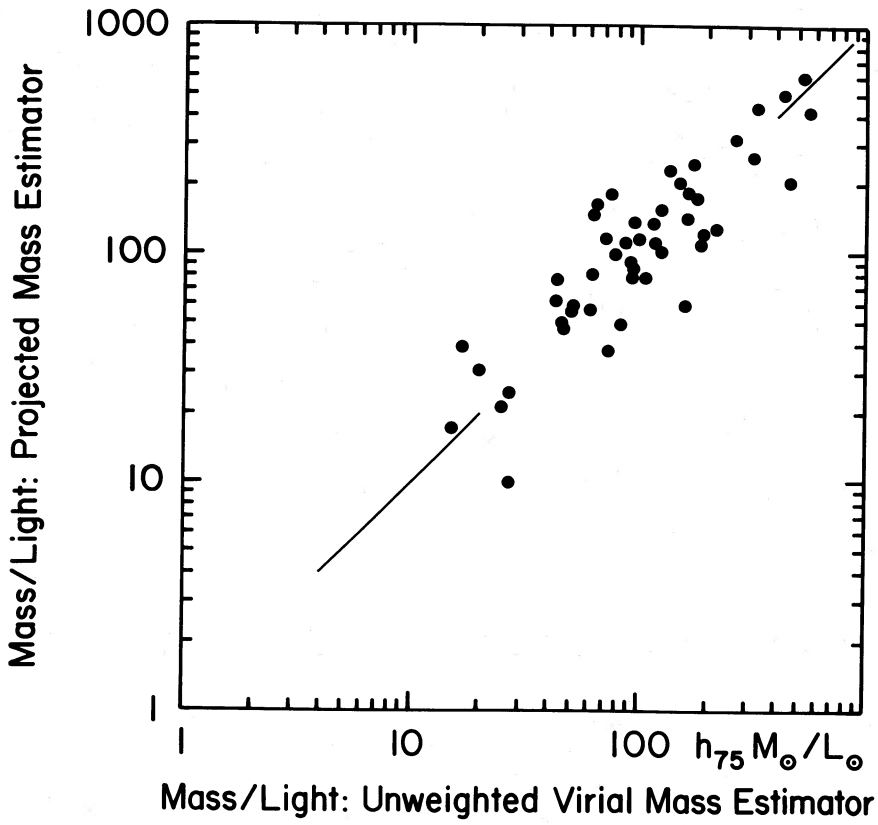

FIG. 8.—Comparison of mass estimators: "projected mass" vs. unweighted virial masses

NBG catalog. For galaxies with unknown luminosities, estimates were made based on dimensions and an assumed global surface brightness of 24.2 mag s^{-2}. There are relatively few of these estimated luminosities, and they are usually for intrinsically small systems, so these poor luminosities do not add much uncertainty.

There has been a correction applied to the integrated luminosities of groups to account for incompletion as a function of distance. As will be described in another place, our sample accommodates a Schechter (1976) luminosity function with $\alpha = -1.00$ and $M^* = -20.18$ ($H_0 = 75$ km s^{-1} Mpc^{-1}). This function has been fit to data in separate distance bins to establish the incompletion as a function of distance. The empirical incompletion correction factor is

$$f = \exp\,[0.045(\mathrm{dm} - 30.0)^{2.82}]\,, \qquad (5)$$

where dm is the distance modulus and $f = 1.0$ if $\mathrm{dm} < 30.0$. Incompletion is substantial at the edge of the NBG catalog at $40h_{75}^{-1}$ Mpc (where $f = 2.7$) but not at the limit of $25h_{75}^{-1}$ Mpc of the analyzed sample (where $f = 1.37$).

Mass-to-light ratios are plotted in Figure 9 for the nearby 179 groups. The median value for the 49 largest groups is $94h_{75}$ $M_\odot/L_\odot$. An alternative scale is provided that is independent of the distance scale: $M_V/L_B^{b,i}$ is replaced by the parameter Ω_g, the mass density associated with groups as a fraction of the critical density required for closure of the universe. The conversion to this scale assumes that $M_V/L_B^{b,i}$ (closure) = $1200h_{75}$ $M_\odot/L_\odot$ (Davis and Huchra 1982: with a 40% adjustment because we include an obscuration correction). The median value of this parameter is $\Omega_g = 0.08$ for the 49 largest groups.

These median values of M/L and Ω_g are about a factor of 2 smaller than the corresponding values found by HG in their analysis of Shapley-Ames galaxies (by the way, we have been comparing our results with HG because it is the most extensive group catalog to cover a similar range of distances as we cover). It may be surprising that the difference between our median and the HG median is only a factor of 2.4, since their median velocity dispersion squared is larger by a factor of 3.2 and their medium virial radius is larger by about a factor of 1.7. However, HG are typically sampling *more luminous* groups than ours. They are sampling groups over a somewhat larger volume and exclude many of the groups composed of low surface brightness systems that we have picked up.

f) Minimum Mass-to-Light Values

Because of uncertainties in deprojected velocities and the applicability of the virial theorem, it is worth mentioning an independent argument that M/L values are typically large. If only the assumption is made that the groups that have been defined have collapsed, then equation (4) can be used to determine the minimum masses required to drive collapse in a Hubble time. The only measured quantity required for each group is the virial radius.

It is seen in Figure 10 that these "minimum" M/L values are usually large, with a median value of 50 $M_\odot/L_\odot$ for the 49 large, nearby groups. Groups that collapsed in a time much shorter than the Hubble time must have values larger than the minimum M/L.

There is a partial redundancy between Figures 3, 9, and 10 in the sense that, given any two, the third could be anticipated. The fact that there is the expected agreement provides some confirmation for both the assumption that our groups have collapsed and the assumption that the virial theorem gives

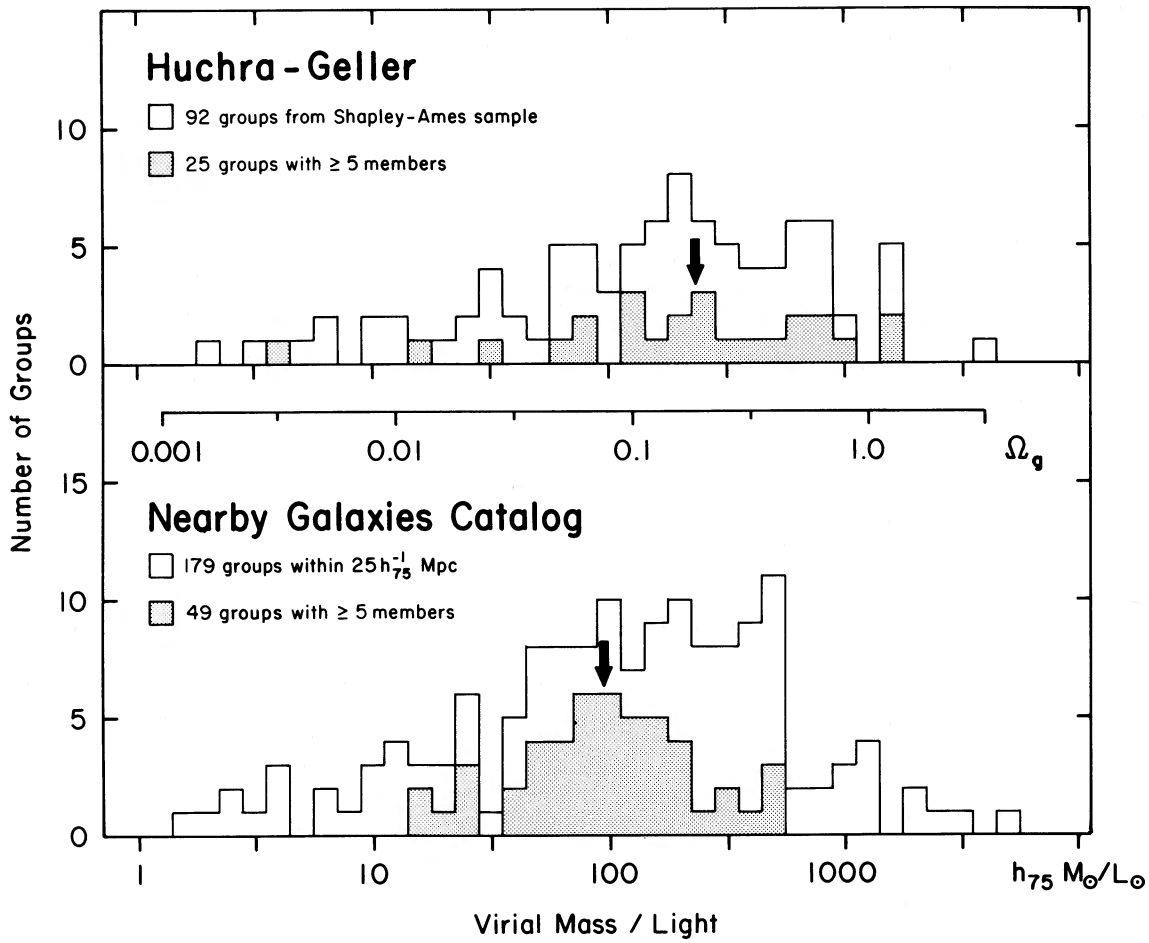

FIG. 9.—Mass-to-light ratios. The bottom panel illustrates the distribution of $M_V/L_B^{b,i}$ values for NBG catalog groups within $25h_{75}^{-1}$ Mpc. The median value of 94 $M_\odot/L_\odot$ for the groups with ≥five members is indicated by the arrow. The equivalent information for the HG Shapley-Ames sample is shown in the top panel, and the arrow locates the median value of 220 $M_\odot/L_\odot$ for the groups with ≥five members.

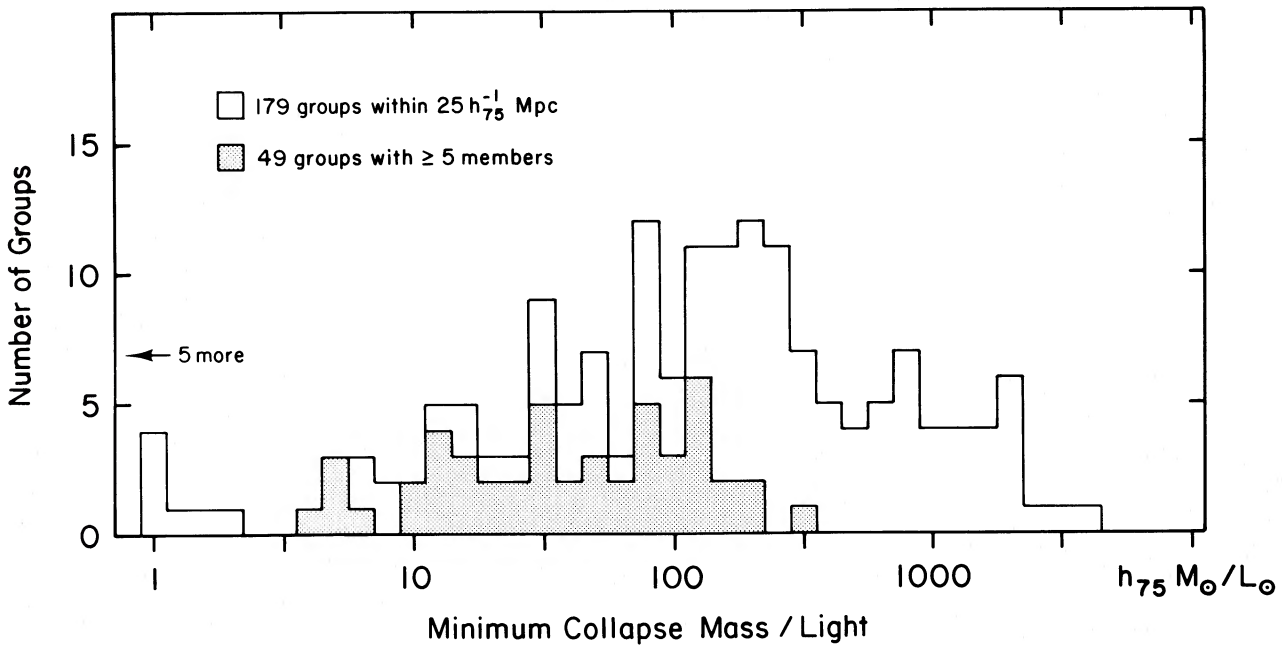

FIG. 10.—Minimum mass-to-light ratios if groups have collapsed. The histograms provide an estimate of masses required if $t_c = H_0^{-1}$ for all the groups identified within a distance of $25h_{75}^{-1}$ Mpc.

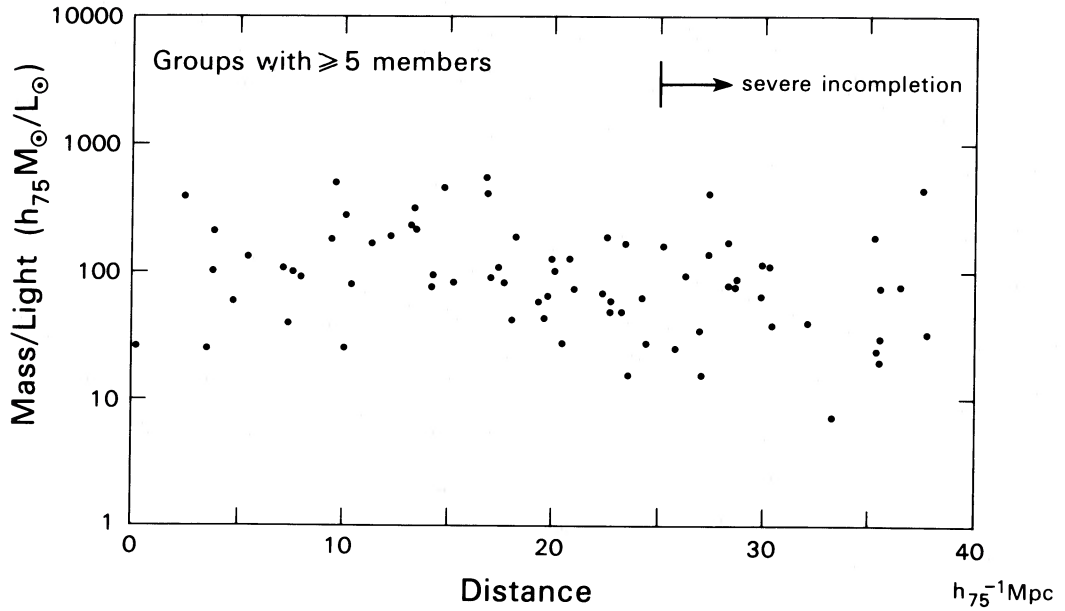

FIG. 11.—Mass-to-light ratios as a function of distance. Values are plotted for all groups with five or more members identified in the NBG catalog.

reasonable mass estimates.

g) Systematics of M/L Values

This discussion will be brief but we should at least touch on some issues that have come up in the past. In the first place, it is to be hoped that our M/L values are not a function of distance. Actually, Figure 11 suggests that they are: M/L appears to *decrease* slightly with distance.

It turns out that if the correction for luminosity incompletion as a function of distance had not been made, then M/L *would* be independent of distance. Yet the correction seems justified. Probably, there is a corresponding distance effect in masses because there are low-luminosity systems that are preferentially lost at large distances that would tend to increase both velocity dispersions and virial radii. In any event, the data in Figure 11 suggest that the deficiency is negligible within $25h_{75}^{-1}$ Mpc, and the analysis of this paper is restricted to groups within this radius.

As is seen in Figure 12, there is a slight indication of a correlation between M/L and R_V. In the decade in R_V from 100 kpc to 1 Mpc, M/L seems to increase by a factor of 3, from 50 to 150. There has been controversy on this issue in the past (Rood, Rothman, and Turnrose 1970; Turner and Sargent 1974; Rood and Dickel 1978). Although tentative, it is unlikely that the present correlation is an artifact of errors in R_V.

There are two points to be made: (1) An increase in mass $M(R) \approx R$ seems required over the interval 10–100 kpc to attain the high values of M/L observed on scales of 100–200 kpc. (2) Mass must increase more *slowly* with radius in the interval 100 kpc to 1 Mpc. Tentatively, the weak correlation seen in Figure 12 suggests $M(R) \approx R^{1/2}$ for 100 kpc $< R <$ 1 Mpc. The curve superposed on Figure 12 illustrates the growth of M/L assuming $M/L = 5$ on a scale of 10 kpc and these dependencies on R.

Finally, it can be asked if the scatter in M/L values is observational or intrinsic. Heisler, Tremaine, and Bahcall (1985) found from n-body simulations that the observational scatter with groups of five was 0.5 in log M/L between the first and third quartiles and, for groups of 10, dropped to 0.3. We observe a first-to-third-quartile scatter that is 0.8 for 128 groups of two to four, 0.5 for 24 groups of five to eight, and still 0.5 for 26 groups of nine or more. The scatter for the groups of smaller than five must be observational, but it is possible that we are beginning to see intrinsic scatter with the largest groups. This upper limit, or possible detection of intrinsic scatter, corresponds to a standard deviation of roughly a factor of two.

V. CONCLUDING REMARKS

The results of group analyses have been notoriously ambiguous in the past because one could have little confidence that many of the groups under study were really bound, or that all relevant members had been included, or that there was not a serious problem with interlopers. These problems caused Faber and Gallagher (1979), in an otherwise incisive review, to comment "we strongly believe that it will never be possible to assign individual galaxies to groups or fields in a definitive way. Any [such] approach ... cannot possibly yield reliable results." Assuming "definitive" still allows for some mistakes, then this viewpoint is unduly pessimistic. The group identification process can be less ambiguous than has been thought. The claim being made here is that the aforementioned problems are much less severe in the present study. This new work incorporated a better understanding of the environments of groups and demands an accounting of every galaxy in the sample. The group selections were done with an automatic algorithm, but all 2367 decisions the computer made were considered subjectively to see if each made sense. Ninety-seven percent did. It is encouraging that such parameters as the dimensions and velocity dispersions of the newly defined groups show less scatter than was apparent with previous investigations.

In the past, the velocity dispersions of groups were typically found to be much larger than our median value of 100 km s^{-1}. For example, Rood and Dickel (1978) found a median value of 250 km s^{-1} for Sandage-Tammann groups and a median value of 190 km s^{-1} for Turner-Gott groups. As previously cited, Huchra and Geller (1982) obtained a median dispersion of 180 km s^{-1} for groups with at least five members. Davis and Peebles (1983) measured a differential velocity between pairs that reduces to a one-dimensional velocity dispersion per galaxy of 210 km s^{-1} at separations of $300h_{75}^{-1}$ kpc. These

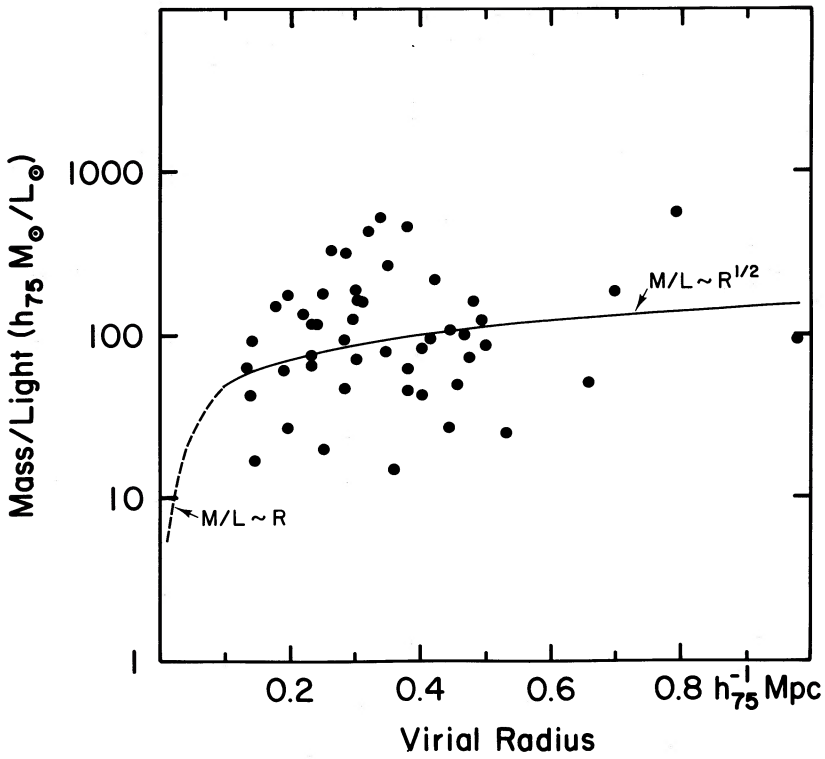

FIG. 12.—Mass-to-light ratios as a function of radius. The data that is plotted is for the 49 groups with ≥five members within $25h_{75}^{-1}$ Mpc. The curves schematically illustrate that the data suggests M/L grows rapidly for $R < 100$ kpc and more slowly, if at all, for $R > 100$ kpc. The dashed curve begins at $M/L = 5\ M_\odot/L_\odot$ at 10 kpc and increased as $M/L \approx R$ out to $R = 100$ kpc. The solid curve grows from this point as $M/L \approx R^{1/2}$.

high values of velocity dispersions almost certainly suffer from interloper contamination. Since groups are in filaments and, sometimes, filaments align close to the line of sight, contamination problems can be severe and not amenable to statistical evaluation. Tammann and Kraan (1978), Karachentsev (1980), and Rivolo and Yahil (1981) are among those who have argued that velocity dispersions have frequently been overestimated.

In spite of these results, we get *high* M/L values. Our luminosities are typically low because our sample is dominated by sparse groups. This result has to be taken as serious evidence for dark matter on a scale of 0.5 Mpc around the average galaxy. The 179 groups within $25h_{75}^{-1}$ Mpc include 69% of the galaxies and 77% of the light in this uniformly sampled volume (the percentage of the light is higher because high-luminosity galaxies are more prone to cluster). Hence the statement that the median $M_V/L_B^{b,i}$ is around 90 $M_\odot/L_\odot$ on a median scale of 0.34 kpc is a statement pertinent to the average galaxy in a completely surveyed volume. This large M/L value is consistent with a roughly linear increase in mass with radius from the scale of the luminous parts of galaxies to the scale of groups (although, as was discussed in the previous section, there may be evidence for a slower increase in mass with radius on scales above 100 kpc). Such extensive halos about galaxies in groups presumably must be merged to a significant degree. Because $M_V/L_B^{b,i} \approx 90\ M_\odot/L_\odot$ can be associated with the average galaxy, a rather firm *lower limit* can be set for the mass density of the universe at $\Omega_g = 0.08$. These conclusions are quite different from those drawn by Valtonen and Byrd (1986) even though their criticisms of previous group analyses are probably valid. Just because previous group identifications had serious interloper problems does not mean that bound groups are not a prominent component of large-scale structure.

There are unanswered questions. For example, what would be the effect of a change of, say, a factor of 3 in the choice of the density threshold that leads to the definition of groups? We plan to examine the matter, and also consider the impact of different choices of the parameter V_l, in a third paper in this series. Are associations and clouds unbound as their low densities and apparently close to free expansion would imply? But if clouds are falling apart, how can the regions between clouds be so deficient in galaxies? Extreme biasing in the galaxy formation process might be implied.

Over the many years since this work began, Herb Rood has been especially helpful with his encouragement that involved subtle threats to do the job himself if I did not get on with it. This research has been supported by NSF grant AST 83-19951.

APPENDIX A

CROSS-REFERENCE BETWEEN GROUP CATALOGS

Table 3 provides a cross-reference between groups identified in the NBG catalog and previous group catalogs. There are at least two galaxies in common between each cross-referenced group. The group catalogs considered are dV = de Vaucouleurs (1975), TG = Turner and Gott (1976), HG = Huchra and Geller (1982), and GH = Geller and Huchra (1983).

TABLE 3

CORRESPONDENCE WITH OTHER GROUP CATALOGS

Group	GH	HG	TG	dV	
11 -1	106	41	57	18,19,20,25	Virgo
11 -4	106	41	57	...	
11 -8	...	41	...	...	
11-10	...	41	...	...	
11-11	...	41	...	...	
11-12	...	41	...	...	
11-14	...	41	...	35	
11-17	...	41	...	...	
11-18	...	41	...	...	
11-21	...	35	...	...	
11-22	...	31	...	...	
11-24	106	41	57	46	Virgo W
11-30	...	42	...	...	
11-35	...	26	...	...	
12 -1	94	60	47,50,51	10,32,34	Ursa Major
12 -2	94	60	47	...	
12 -3	94	60	47	...	
12 -5	94	60,82	47	...	
12 -6	94	60	52	17	
12 -8	64	...	...	...	
12 -9	63	...	...	...	
12-10	...	91	...	...	
12-12	94	60	47	...	
12-13	94	60	31	28	
12-16	94	60	47		
13 -1	...	...	18	...	
13 -5	46	...	6	41	
13 -6	...	80	...	41	
13 -7	84	...	...	...	
13 -8	79	...	41	...	
13 -9	...	...	49	...	
14 -1	94	60	53	13	Coma I
14 -2	94	60	64	...	
14 -4	94	60	50,62	10	CVn II
14 -5	116	...	72	5	
14 -6	94	60	61	10	
14 -7	94	60	54	3	CVn I
14 -9	128	75	82	9	M 101
14-10	52	85,86	16	2	M 81
14-11	...	84	...	...	IC 342
14-12	...	63	...	...	Local
14-13	...	13	...	1	Sculptor
14-15	...	19	...	4	Centaurus
15 -1	68	56	27	11	M 96
15 -2	78	56	38	9	
15 -4	...	...	33	...	
15 -9	75	...	...	...	
15-10	...	74	...	6	
15-11	...	71	...	6	
17 -1	...	67	...	7	
17 -4	17	...	...	...	
17 -5	22	58	...	...	
19 -1	...	2	...	...	
19 -3	...	...	...	14	
19 -6	...	15	...	...	
19 -8	...	13	...	...	
21 -1	77	56	39	49	
21 -3	68	56	...	11	
21 -5	68	56	27	...	
21 -6	58,61	57	21,25	47	
21 -7	71	61	33	48	
21 -8	60	62	...	54	
21 -9	67	65	28	43	
21-10	57	54	20	...	
21-11	76	53	40	...	
21-12	50	64	11,13	42	
21-13	51	...	15	...	
21-15	43	...	...	...	
21-16	45	...	...	...	
21-17	45	...	7	...	
21-18	43	66	...	...	
22 -1	...	33	...	...	
22 -4	...	28	...	44	
22 -5	...	27	...	44	
22 -7	...	...	...	23	
22-11	100	51	57	...	
23 -1	...	14	...	...	
23 -5	...	20	...	...	
31 -2	...	18	...	...	Antlia
31 -3	...	18	...	...	
31 -4	...	21	...	...	
31 -5	...	29	...	...	
31-12	...	36	...	...	
31-14	...	38	...	...	
34 -8	...	34	...	36	
41 -1	150	50	95	50	NGC 5846
41 -2	145,148	49,50	92,95	29	
41 -3	139,145	49	87	...	
41 -7	124	55	79	...	
41-10	...	40	...	...	
41-12	...	46	...	...	
41-13	...	46	...	...	
42 -1	123	69	77	...	NGC 5371
42 -2	...	...	72	...	
42 -3	135	73	91	37	
42 -4	135	72	83	...	
42 -6	132	77	82	...	
42 -7	144	76	...	...	
42 -8	122	81	78	...	
42-13	107	88	58	...	
42-14	99	...	...	...	
42-16	...	92	...	...	
43 -1	115	68	67,69	...	
43 -3	147	...	...	...	
44 -1	152	78	...	30	
44 -8	...	...	...	51	
51 -1	...	17	...	53	Fornax
51 -4	...	32	...	...	NGC 1332
51 -5	...	30	...	...	
51 -7	...	32	...	31	
52 -1	...	44	...	...	
52 -2	32	48	...	15	
52 -3	28	...	...	...	
52 -7	...	45	...	33	
52-11	21	...	...	...	
52-12	12	52	...	40	
52-15	20	...	...	...	
53 -1	...	3	...	16	NGC 1566
53 -2	...	3	...	...	
53 -3	...	3	...	22	
53 -4	...	3	...	...	
53 -7	...	8	...	21	
53 -8	...	6	...	...	
53-10	...	16	...	...	
53-13	...	25	...	...	
53-17	...	1	...	...	
54 -3	...	...	...	8	
61 -1	...	9	...	52	NGC 6868
61 -2	...	...	...	52	
61 -6	...	11	...	...	
61-11	...	10	...	...	
61-12	...	7	...	...	
61-16	...	12	...	27	
61-18	...	...	...	39	
61-19	...	...	...	39	
64 -1	163	...	...	...	
64 -7	175	...	...	...	
71 -1	156	...	98	...	
72 -1	153	...	...	...	

APPENDIX B

ELABORATION ON THE GROUP-FINDING PROCEDURE: THE LEO REGION

As a clarification of the manner in which groups are identified, it is instructive to look in some detail at what was done in a small region. We can evaluate whether there is sensitivity to the adjustable parameters and compare results with earlier investigations. The Leo region is worth consideration. The analysis of this region must confront one special problem, but once that problem has been surmounted, further interpretation becomes quite straightforward.

In the maps given by Tully (1982), three clouds seem to converge in Leo: the units at that time called Leo I, Leo II, and Leo Minor. These maps were based on the assumption of a uniform Hubble flow. It is now generally accepted that the Virgo Cluster has a significant effect on the local velocity field. Tully and Shaya (1984) discussed a model that conforms to available information about velocity perturbations in the Local Supercluster. In this specific model, the present zero-expansion surface about the Virgo Cluster subtends a radius of 28° and reaches to approximately the halfway point between the Virgo Cluster and our Galaxy.

The parts of the clouds of galaxies in Leo that lie nearest to the Virgo Cluster are viewed in projection near the edge of the zero-expansion surface. The prediction of the Virgo infall model is that there would be very small changes in velocity over considerable distances in the line-of-sight in this region. This prediction is confirmed by observations. Distances to individual galaxies can be estimated using the techniques and calibrations discussed by Tully and Shaya (1984). It is evident that the galaxies associated with what was called the Leo I and Leo Minor clouds (now called the Leo Spur) are at less than half the distance of what was called the Leo II Cloud (now simply called the Leo Cloud).

The special problem, then, is to get assignments right between the foreground Leo Spur and the background Leo Cloud in a situation where there is poor velocity discrimination. Even farther to the background, there is another cloud of galaxies called the

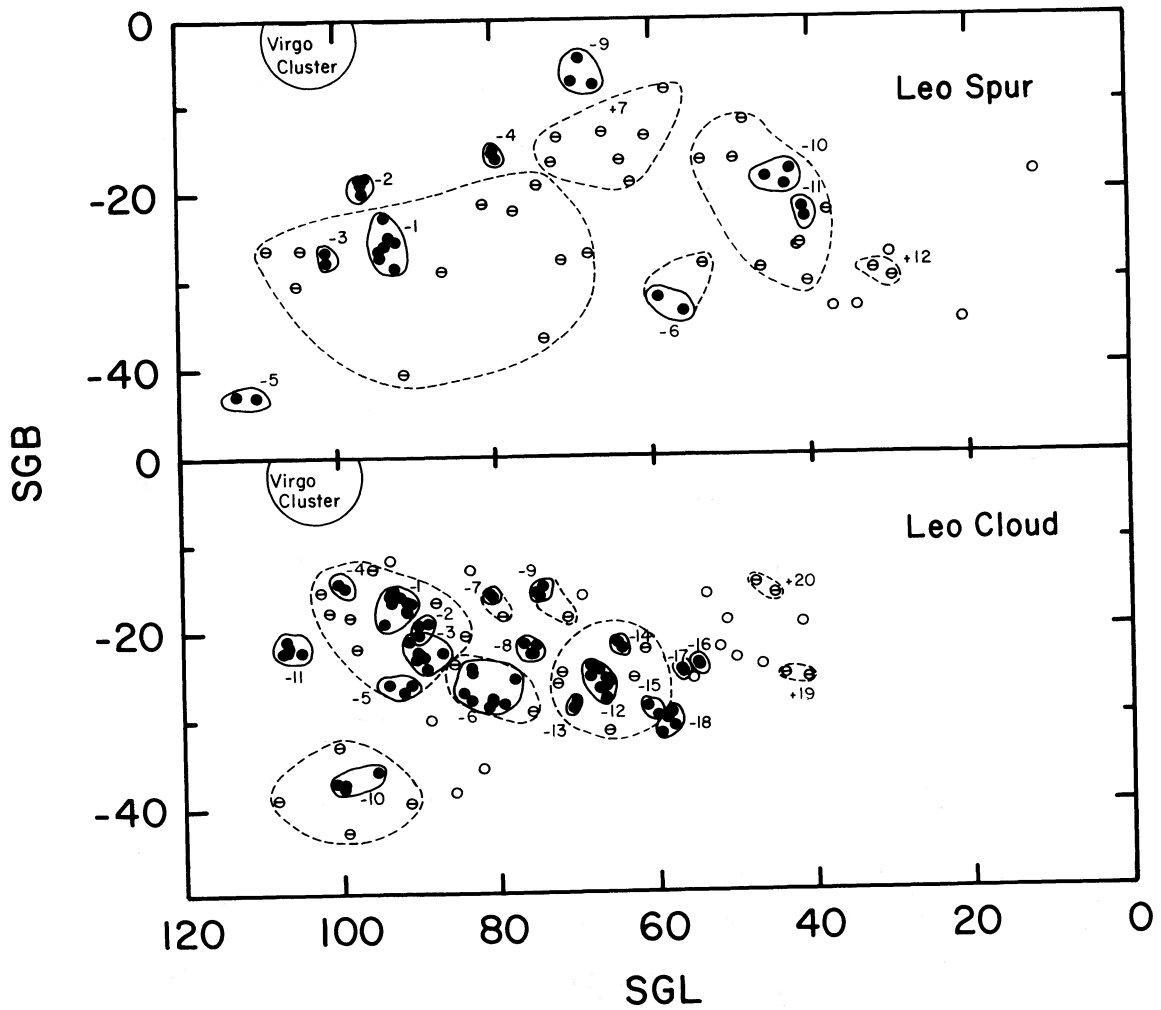

FIG. 13.—Distribution on the plane of the sky of galaxies in the Leo Spur and Leo Cloud. (*filled circles*) Galaxies in groups. Solid contours outline groups. Negative numbers are group names. (*divided circles*) Galaxies in associations. Dashed contours outline associations. Positive numbers are association names. (*open circles*) Galaxies at large in clouds. (*top panel*) Leo Spur. Cloud prefix to group name is 15. (*Bottom panel*) Leo Cloud. Cloud prefix to group name is 21.

TABLE 4

COMPARISON WITH HUCHRA-GELLER (SHAPLEY-AMES SAMPLE)

Name (1)	Number (2)	V (3)	R (4)	M/L (5)	Comments (6)
HG 53.....	4	139	0.52	324	
21−11.....	5	129	0.38	159	HG: N3611, N3630, N3640, N3664 add: U6345
HG 54	3	25	0.13	3	
21−10	5	61	0.20	27	HG: N3156, N3166, N3169 add: U5522, U5539
HG 56	30	251	1.19	251	Three not in NBG
15−1	9	112	0.14	90	HG: N3351, N3368, N3377, N3379, N3384, N3412, N3489 add: N3299, U5889
15−2	4	97	0.09	44	HG: N3593, N3623, N3627, N3628
21−1	11	220	0.31	166	HG: N3596, N3607, N3608, N3626, N3655, N3681, N3684, N3686 add: N3605, N3659, U6320
21−3	10	98	0.23	73	HG: N3370, N3455, N3507 add: N3443, N3447, N3454, U5947, U6007, U6035, U6112
21−5	3	9	0.68	2	HG: N3338, N3346, N3389
21+4	...	...	...	...	HG N3666, N3705 add: three more
HG 57	6	184	0.19	141	One not in NBG; One in 15−0
21−6	12	124	0.29	68	HG: N3162, N3193, N3226, N3227 add: N3177, N3185, N3187, N3190, N3287, N3301, U5588, U5675
HG 61	3	77	0.29	47	One in 21+7
21−7	2	95	0.08	39	HG: N3504, N3512
HG 62	3	77	0.67	141	
21−8	4	72	0.20	37	HG: N3245, N3254, N3277 add: U5662
HG 64	3	95	1.40	537	
21−12	10	88	0.37	62	HG: N2964, N3003, N3067 add: N2968, N2970, N3011, N3021, U5393, 0945+33, 0954+33
HG 65	6	81	0.13	16	Two not in NBG
21−9	4	67	0.06	6	HG: N3395, N3396, N3430, N3442
HG 66	3	170	1.87	831	One in 21−15
21−18	5	122	0.33	110	HG: N2770, N2778 add: N2780, U4777, U4837
HG 71	4	56	0.65	389	Two in 15+11
15−11	2	11	0.22	12	HG: N2541, N2552
HG 74	3	121	1.32	676	One not in NBG; One in 15+10
15−10	3	...	0.54	...	HG: N2681 add: U4499, U4514

COL. (1).—Catalog number in HG, followed by the corresponding entries in the NBG catalog.

COL. (2).—Number of group members.

COL. (3).—Velocity dispersion. The NBG values have been adjusted for measurement errors, but the HG values have not been adjusted.

COL. (4).—Harmonic radius for the HG groups or virial radius for the NBG groups. The HG values are adjusted to be consistent with $H_0 = 75$ km s^{-1} Mpc^{-1}.

COL. (5).—Mass-to-light ratio. The HG value is adjusted to be consistent with $H_0 = 75$ km s^{-1} Mpc^{-1} and the luminosity corrections used in this paper.

COL. (6).—With the available information, the composition of the NBG groups can be reconstructed and the differences between the two group catalogs can be determined.

Leo-Cancer Cloud, but this entity is cleanly separated in velocity. Over the entire region of sky that encloses these three structures in projection, the only galaxies with $V_0 < 3000$ km s^{-1} *not* associated with one of these three structures are dwarf galaxies in the Local Group.

The procedure followed to achieve the separation between the Leo Spur and the Leo Cloud is as follows. As a first approximation, distances were assigned in accordance with the Virgo infall model. Along a given line-of-sight, any galaxy with a systemic velocity less than a certain value would have been placed to the foreground, and any galaxy with a velocity that was larger would be placed in the background. Then all galaxies with systemic velocities within a few hundred kilometers per second of the critical velocity were reconsidered. Distances were estimated to individual galaxies using the methods described by Tully and Shaya (1984), and galaxies were placed in the foreground or background in accordance with the results. Finally, all projected tight knots of galaxies were considered, and the demand was made that all galaxies within a knot be assigned to the same background or foreground cloud. Distance estimates were almost always available to some members of the knots.

Once the cloud assignments have been made, the group-finding procedure was straightforward to apply in the Leo region. In Figure 13, one can see the projected distribution of galaxies in each of the two entities, the Leo Spur and the Leo Cloud. Both of these features happen to stretch out close to the plane of the sky and, as a consequence, there is almost no intracloud confusion problem due to projection effects.

This point is important. Since there are virtually no projection problems, there is *no sensitivity* on the high side to the choice of the parameter V_l. If a larger value of V_l is chosen, the groups 21 − 2 and 21 − 3 could be merged and, similarly, so could groups 21 − 15 and 21 − 18. Otherwise, *any value* of V_l greater than 300 km s^{-1} would produce the same results.

The qualitative basis for our description in terms of groups and associations can be seen in the distribution of galaxies in Figure 13. It can be seen that there are tight knots in a sea of apparently unbound systems. Together, these two clouds are reasonably typical, with 117 galaxies (62%) in 27 groups, 53 galaxies (28%) in associations, and 19 galaxies (10%) at large.

There is one characteristic of the distribution of galaxies that can be seen in the nearby Leo Spur but that would not be observable with the present data set at the distance of the Leo Cloud. There are entities we call associations, like 15 + 7 and 15 + 10, that contain mostly small, low-surface-brightness galaxies. These entities can have density contrasts that suggest they are physically significant, but the regions are very unlikely to be bound given the tidal shears they experience.

We will now compare our group catalog of the Leo region with the HG and GH catalogs. The comparisons in the rest of this paper have generally been with HG because that work was based on the all-sky Shapley-Ames sample. The catalog by GH is based on the deeper CfA sample. Materne (1978) has also done a group analysis specifically on the Leo region.

We begin with a comparison with HG. The major difference results from what we claim is confusion caused by the projection of the Leo Spur onto the Leo Cloud in the vicinity of SGL $\approx 92°$, SGB $\approx -24°$. Because of the consequent high density in this area, HG joined five of our groups together, including two from the Leo Spur and three from the Leo Cloud. As a result, HG obtain high values for the velocity dispersion, harmonic radius, and M/L for this important group. Detailed differences between us are outlined in Table 4.

TABLE 5

COMPARISON WITH GELLER-HUCHRA (CfA SAMPLE)

GH Catalog Number	Number of Members in GH Group	NBG Group Catalog Number[a]	Number of Members in NBG Group	Number of Galaxies in Common[b]	Number of GH Galaxies Not in NBG Catalog
GH 43.....	5	21−15	2	2	0
		21−18	5	3	
GH 45.....	4	21−16	2	2	0
		21−17	3	2	
GH 50.....	8	21−12	10	6	2
GH 51.....	3	21−13	2	2	1
GH 57.....	4	21−10	5	3	1
GH 58.....	10	21−6	12	9	3
GH 61.....	3	15−0	...	1	
GH 60.....	4	21−8	4	3	1
GH 67.....	8	21−9	4	4	4
GH 68.....	23	15−1	9	8	6
		21−2	3	1	
		21−3	10	5	
		21−5	3	3	
GH 71.....	7	21−7	2	2	4
		21+7	...	1	
GH 75.....	3	15−9	3	3	0
GH 76.....	7	21−11	5	5	2
GH 77.....	13	21−1	11	10	3
GH 78.....	9	15−2	4	4	2
		21−1	11	1	
		21+4	...	2	

[a] Corresponding entry in NBG group catalog. In cases with brackets, there are multiple correspondences.

[b] Number of galaxies in common to the GH and NBG group catalogs.

Otherwise, there are only minor differences between HG and the present group assignments, though as seen in Table 4, the M/L values determined in this paper tend to be lower. We do not understand what led to the definition of HG 57 and HG 64. The harmonic radius associated with HG 62 is probably too big.

The CfA group catalog by GH did not include a tabulation of M/L values, so we make a less detailed comparison with this work. The major difference is again in the way the region around SGL $\approx 92°$, SGB $\approx -24°$ is handled. The GH 68 group has 23 members that we allocated to one group in the Leo Spur and three groups in the Leo Cloud. Table 5 provides an abbreviated summary of the correspondence between GH and the present group assignments in the Leo region.

The Leo region is representative of the present catalog. There was a special problem in the analysis of this region because it lies near the tangent point of the Virgo zero-velocity surface. This problem does not hamper the analysis in most other regions. On the other hand, the Leo region is favorable because, conveniently, the individual filamentary clouds have relatively little depth from our viewing position. There are other situations that are difficult because we happen to be aligned close to the major axis of elongated structure. Confusion can be more of a problem in these cases. Fortunately, a good value for the parameter V_l can be determined in situations where the geometry is clean, such as in the Leo region, and can be applied with confidence to the more confused regions. The basic characteristics of the groups that are subsequently defined are consistent in different parts of the sky.

REFERENCES

Arp, H. 1970, *Nature*, **225**, 1033.
Arp, H., and Sulentic, J. W. 1985, *Ap. J.*, **291**, 88.
Bahcall, J. N., and Tremaine, S. 1981, *Ap. J.*, **244**, 805.
Byrd, G. G., and Valtonen, M. J. 1985, *Ap. J.*, **289**, 535.
Chamaraux, P., van Woerden, H., Goss, W. M., Mebold, U., and Tully, R. B. 1999, in preparation.
Davis, M., and Huchra, J. P. 1982, *Ap. J.*, **254**, 437.
Davis, M., and Peebles, P. J. E. 1983, *Ap. J.*, **267**, 465.
de Vaucouleurs, G. 1975, in *Stars and Stellar Systems*, Vol. **9**, *Galaxies and the Universe*, ed. A. Sandage, M. Sandage, and J. Kristian (Chicago: University of Chicago Press), p. 557.
de Vaucouleurs, G., de Vaucouleurs, A., and Corwin, H. G., Jr. 1976, *Second Reference Catalogue of Bright Galaxies* (Austin: University of Texas Press).
Faber, S. M., and Gallagher, J. S. 1979, *Ann. Rev. Astr. Ap.*, **17**, 135.
Fisher, J. R., and Tully, R. B. 1981, *Ap. J. Suppl.*, **47**, 139.
Geller, M. J., and Huchra, J. P. 1983, *Ap. J. Suppl.*, **52**, 61 (GH).
Gunn, J. E., and Gott, J. R. 1972, *Ap. J.*, **176**, 1.
Heisler, J., Tremaine, S., and Bahcall, J. N. 1985, *Ap. J.*, **298**, 8.
Huchra, J. P., Davis, M., Latham, D., and Tonry, J. 1983, *Ap. J. Suppl.*, **52**, 89.
Huchra, J. P., and Geller, M. J. 1982, *Ap. J.*, **257**, 423 (HG).
Jaakola, T. 1971, *Nature*, **234**, 534.
Jackson, J. C. 1975, *M.N.R.A.S.*, **173**, 41P.
Karachentsev, I. D. 1980, *Astrofizika*, **16**, 217 (1981, *Astrophysics*, **16**, 133).
Materne, J. 1974, *Astr. Ap.*, **33**, 451.
———. 1978, *Astr. Ap.*, **63**, 401.
———. 1979, *Astr. Ap.*, **74**, 235.
Reif, K., Mebold, U., Goss, W. M., van Woerden, H., and Siegman, B. 1982, *Astr. Ap. Suppl.*, **50**, 451.
Rivolo, A. R., and Yahil, A. 1981, *Ap. J.*, **251**, 477.
Rood, H. J. 1983, in *IAU Colloquium 76, The Nearby Stars and the Stellar Luminosity Function*, ed. A. G. D. Philip and A. R. Upgren (Schenectady, NY: L. Davis Press), p. 411.
Rood, H. J., and Dickel, J. R. 1978, *Ap. J.*, **224**, 724.
Rood, H. J., Rothman, V. C. A., and Turnrose, B. E. 1970, *Ap. J.*, **162**, 411.
Sandage, A. 1978, *A.J.*, **83**, 904.
Sandage, A., and Tammann, G. A. 1981, *Revised Shapley-Ames Catalog of Bright Galaxies* (Washington, DC: Carnegie Institution).
Schechter, P. L. 1976, *Ap. J.*, **203**, 297.
Shapley, H., and Ames, A. 1932, *Harvard Ann.*, Vol. **88**, No. 2.
Tammann, G. A., and Kraan, R. 1978, in *IAU Symposium 79, The Large-Scale Structure of the Universe* (Dordrecht: Reidel), p. 71.
Tully, R. B. 1980, *Ap. J.*, **237**, 390 (Paper I).
———. 1982, *Ap. J.*, **257**, 389.
———. 1987, *Nearby Galaxies Catalog* (Cambridge: Cambridge University Press) (NBG catalog).
Tully, R. B., and Fisher, J. R. 1987, *Nearby Galaxies Atlas* (Cambridge: Cambridge University Press) (NBG atlas).
Tully, R. B., and Fouqué, P. 1985, *Ap. J. Suppl.*, **58**, 67.
Tully, R. B., and Shaya, E. J. 1984, *Ap. J.*, **281**, 31.
Turner, E. L., and Gott, J. R. 1976, *Ap. J. Suppl.*, **32**, 409.
Turner, E. L., and Sargent, W. L. W. 1974, *Ap. J.*, **194**, 587.
Valtonen, M. J., and Byrd, G. G. 1986, *Ap. J.*, **303**, 523.
Vennik, J. 1984, *Tartu Astr. Obs. Teated*, No. 73, p. 3.

R. BRENT TULLY: Institute for Astronomy, 2680 Woodlawn Drive, Honolulu, HI 96822